NUREG-0956

INFORMAL REPORT

on

SOURCE TERM PREDICTIONS FOR VARIOUS CONTAINMENT FAILURE ASSUMPTIONS

to

U.S. NUCLEAR REGULATORY COMMISSION

August 29, 1984

by

J. A. Gieseke, H. Chen, P. Cybulskis,
R. Freeman-Kelly, M. R. Kuhlman, and K. W. Lee

BATTELLE
Columbus Laboratories
505 King Avenue
Columbus, Ohio 43201

TABLE OF CONTENTS

LIST OF TABLES

LIST OF FIGURES

LIST OF FIGURES
(Continued)

SOURCE TERM PREDICTIONS FOR VARIOUS CONTAINMENT FAILURE ASSUMPTIONS

by

J. A. Gieseke, H. Chen, P. Cybulskis,
R. Freeman-Kelly, M. R. Kuhlman, and K. W. Lee

August 29, 1984

The fission product release analyses presented in BMI-2104 were based on a variation of the so-called threshold containment failure model. In the threshold failure model, loss of containment function is assumed to take place when the containment loading reaches a preselected level; at the preselected failure load the containment is assumed to fail, frequently by assuming a large opening or even complete loss of the containment function. Since it was recognized that the loadings that may lead to containment failure are not well defined, the BMI-2104 analyses also examined the effect of containment failure for cases where predicted loads only approached the given failure levels without exceeding them.

In the analyses for the Zion design, a containment failure pressure of 149 psia was assumed based on earlier analyses. Since the predicted containment pressures for the Zion accident sequences considered were well below this failure level, it was not felt appropriate to consider containment failure due to structural overloading. Thus in the analyses in BMI-2104 for the Zion design, only nominal containment leakages were explicitly considered. In the analyses for the Surry PWR design, on the other hand, predicted accident containment loadings were frequently close to the assumed failure level of 100 psia, without actually reaching this level; in these instances the analyses were performed by both assuming that the containment fails and assuming that the containment does not fail. Because of the importance to source terms of containment failure times and leak rates, it was believed important to investigate these effects more extensively and in a parametric fashion.

The Containment Performance Working Group (CPWG) was formed by the Nuclear Regulatory Commission to address questions related to the

ability of reactor containments to withstand the loads that may be imposed during severe reactor accidents. While the work of the CPWG is still continuing, among the early outcomes of the work of this Group is the postulate that containments may lose some of their functional capability due to the deterioration of penetration seals before the structural integrity of the containment is challenged. This postulate has led to the "leak before break" model in the form of an increasing leak rate as a function of internal pressure. In this report, the effect on predicted fission product release to the environment of this leak before break model has been explored for the Zion and Surry PWR designs. In addition, the effect on subsequent fission product release of the failure of the containment to isolate in the event of an accident has been evaluated for each of the plant designs considered in BMI-2104 (Surry, Zion, Sequoyah, Peach Bottom, and Grand Gulf). It is important to distinguish between the two types of containment failures considered in these analyses. The containment isolation failure is present at the start of the accident due to a system fault and is not related to the accident environment. The leak before break type of failure that is being postulated is a direct consequence of the accident environment.

While failures of containment isolation are distinctly different from failures due to accident induced pressure and/or temperature loads for the purposes of consequence (source term to the environment) assessment, the former can be a useful point of reference. Failure to isolate is known to have a finite and nonnegligible likelihood of occurrence and is thus of interest in itself. Also, failure to isolate can be a useful surrogate for noncatastrophic failure due to accident loads. It can be viewed in both contexts for the purposes of this study. The analyses performed for each of the plants are discussed below.

The basis for the analyses reported here was consistent for all plants. The containment isolation failure was assumed to be in the form of a preexisting hole 6 inches in diameter. For the "leak before break" cases, the equivalent hole sizes as a function of containment pressure developed by the CPWG were employed for the Zion design and similar assumptions developed by scaling for Surry. The accident

sequences used for each plant are as follows: Zion-TMLB', Surry-TMLB', Sequoyah-TMLB', Peach Bottom-TC, and Grand Gulf-S_2E.

Zion -- Large, Dry PWR

Table 1 presents the equivalent hole size as a function of containment pressure developed by the CPWG for the Zion design and used in these calculations. The containment isolation failure was assumed to take the form of a hole 6 inches in diameter. The analyses to examine the effects of the above containment failure modes were based on the TMLB sequence in the Zion PWR design.

The accident event times for the Zion TMLB' sequence from BMI-2104 are given in Table 2. Figure 1 gives the containment pressure history without any containment degradation. Figures 2 and 3 show the containment pressures for the medium and high leaks, respectively, as defined in Table 1. It is seen that leaks of the magnitude considered here have a perceptible, but minimal effect on the predicted containment pressure response. Figure 4 gives the containment pressure response for the assumed failure to isolate. The effect on the containment pressure response is quite dramatic compared to the previous cases. This is because the hole size assumed for the isolation failure is larger than for the leakage cases and because the isolation failure is postulated to exist at the start of the accident rather than developing in response to the accident loads. Figures 5 through 7 present the total volume of gases leaked from the containment for each of the foregoing cases; the differences between the isolation failure case and the leak before break case is again quite obvious.

The above containment responses were used as the basis for evaluating fission product releases to the environment. For the fission product sources in the containment, the release from the primary system as given in Tables 7.3 and Figures 7.5 through 7.8 of BMI-2104, Volume VI, were used since the response of the primary system was essentially unaffected by the changes in the containment response. The source from the core-concrete interaction was as given in Table 6.11 also from BMI-2104, Volume VI.

TABLE 1. TOTAL LEAK AREA ESTIMATED AS A FUNCTION OF CONTAINMENT PRESSURE

Containment Pressure (psia)	Low Leak Area ($in.^2$)	Medium Leak Area ($in.^2$)	High Leak Area ($in.^2$)
Normal Operating (14.7)	0.1	0.5	1.0
38	0.1	0.62	1.48
62	0.1	0.62	1.84
120	0.1	2.13	10.96
149	0.1	5.33	23.72

TABLE 2. ACCIDENT EVENT TIMES, ZION

Event	Time, minutes
Zion-TMLB'-1	
Steam generator dry	82.5
Core uncover	109.8
Start melt	130.5
Start slump	158.5
Core collapse	159.8
Vessel head dry	169.2
Head fail	169.5
Cavity dry	316.4
Concrete attack	389.1
End calculation	1001.8

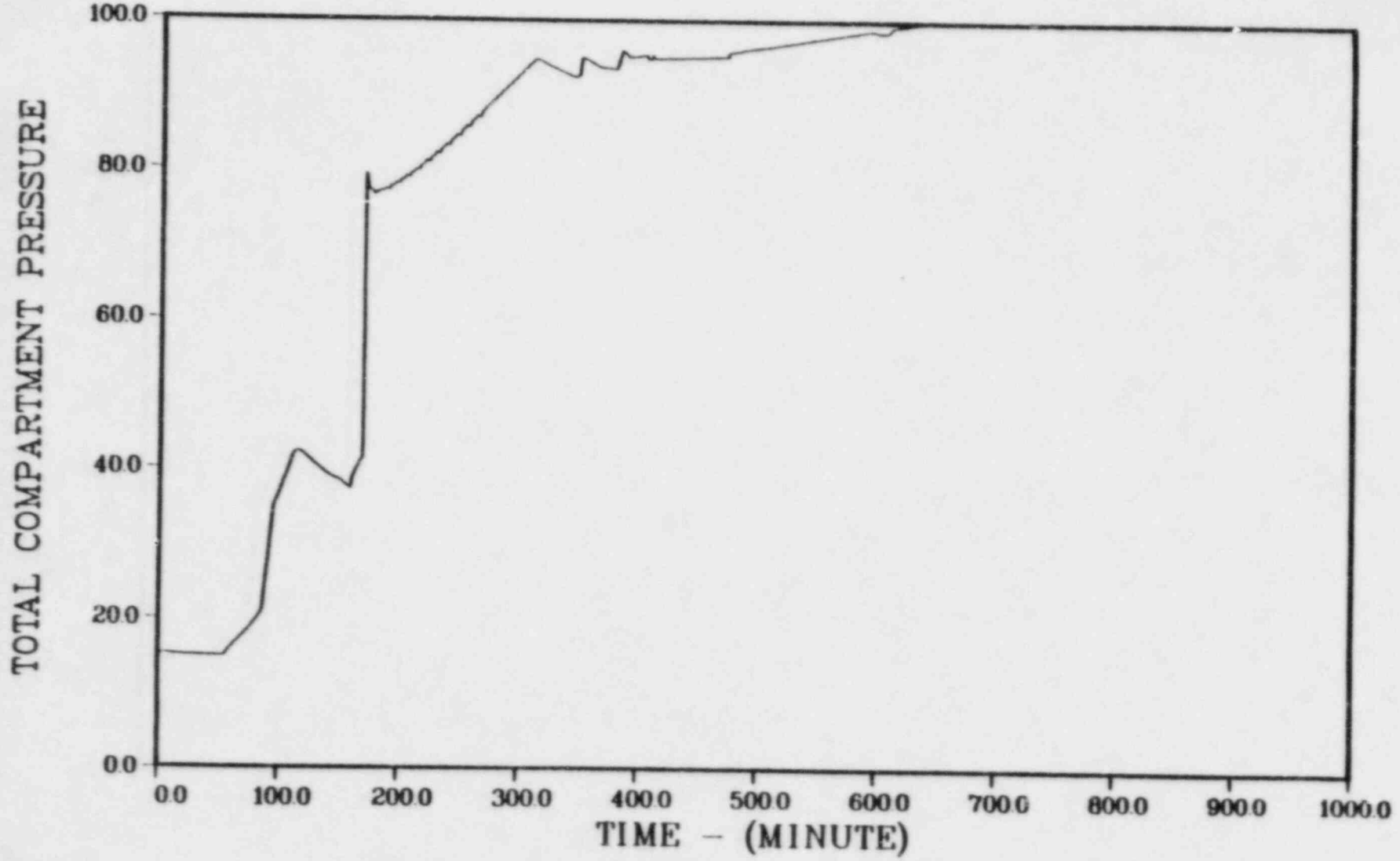

FIGURE 1. CONTAINMENT PRESSURE AS A FUNCTION OF TIME (NO LEAK)

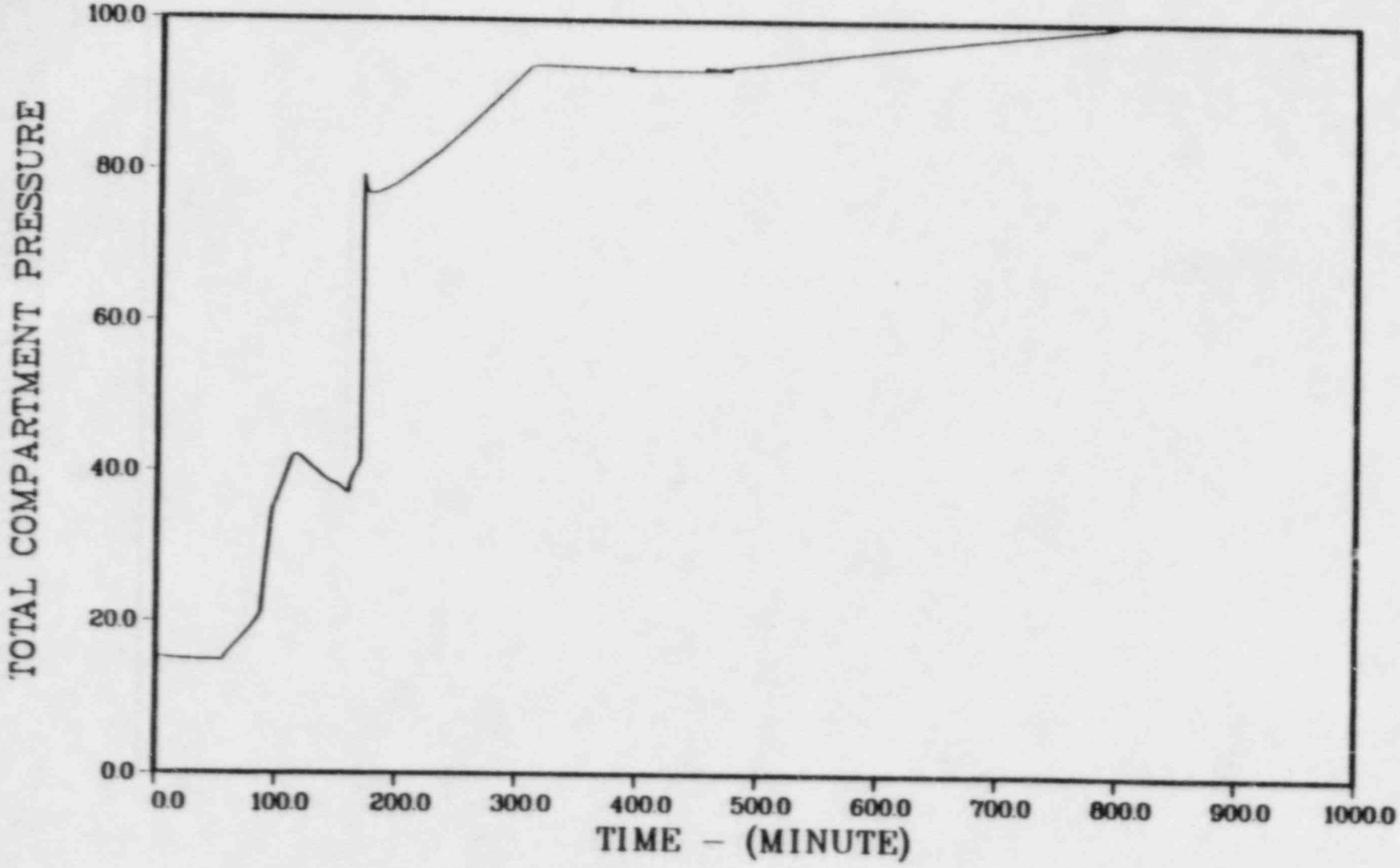

FIGURE 2. CONTAINMENT PRESSURE AS A FUNCTION OF TIME (MEDIUM LEAK)

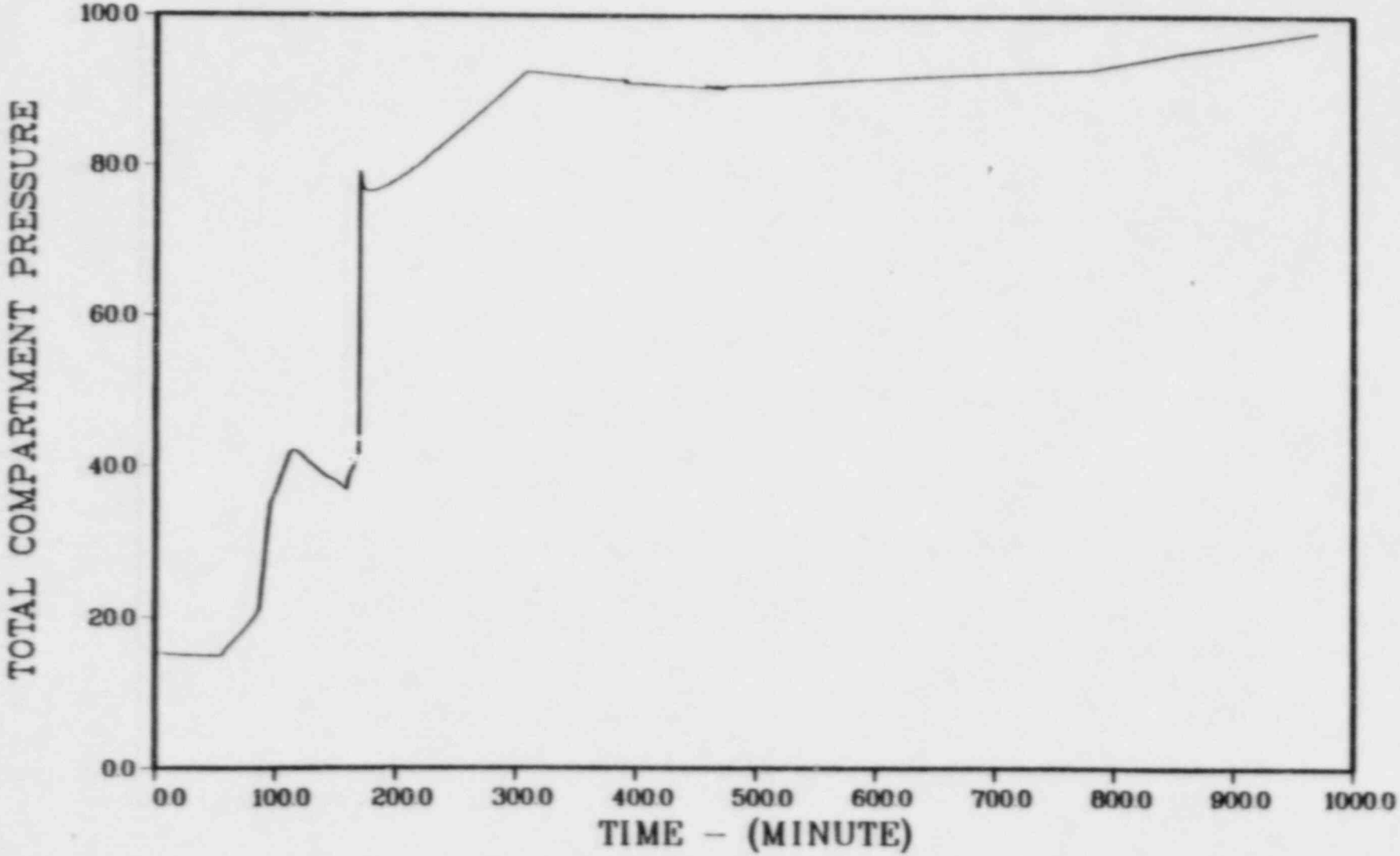

FIGURE 3. CONTAINMENT PRESSURE AS A FUNCTION OF TIME (HIGH LEAK)

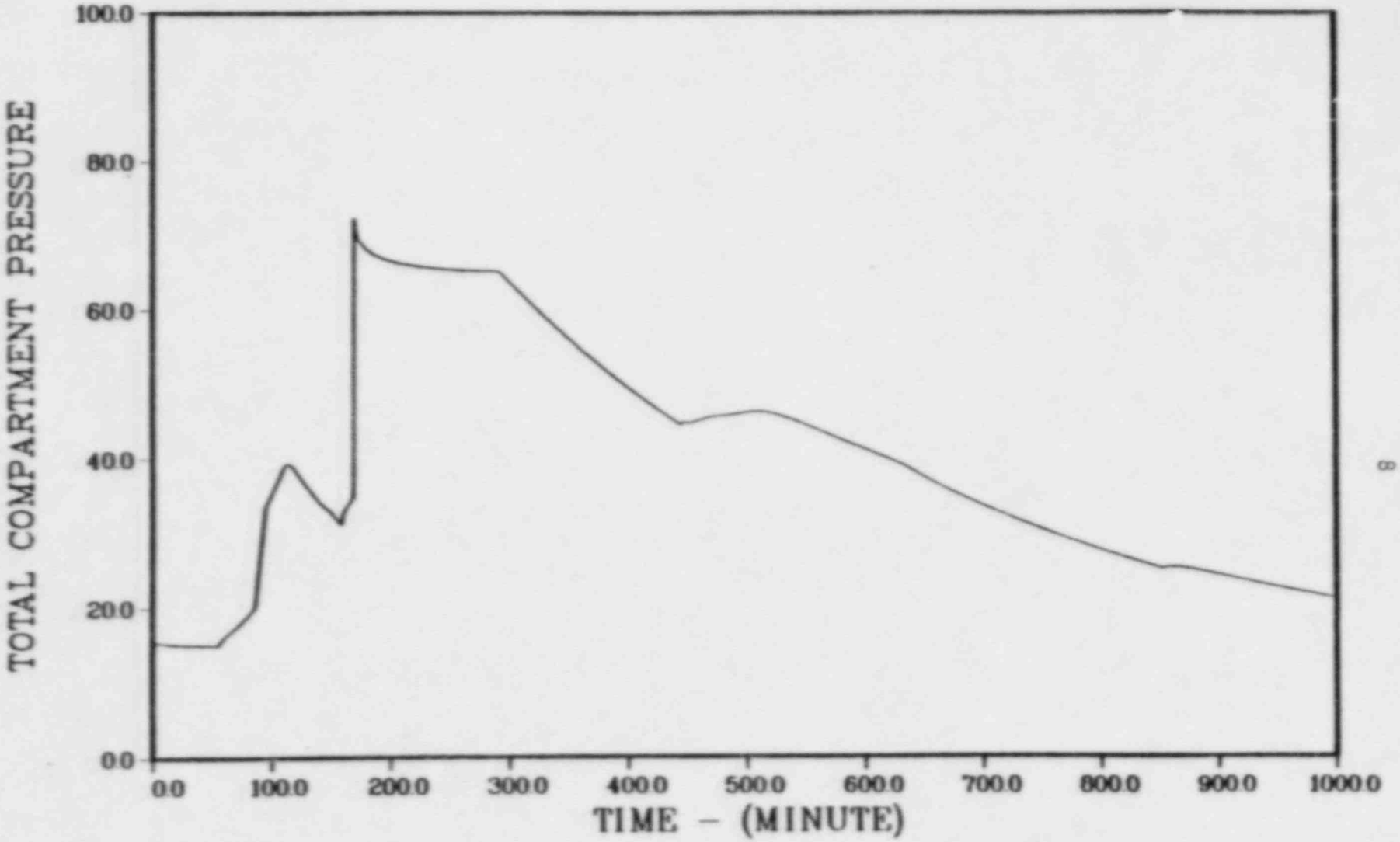

FIGURE 4. CONTAINMENT PRESSURE AS A FUNCTION OF TIME (ISOLATION FAILURE)

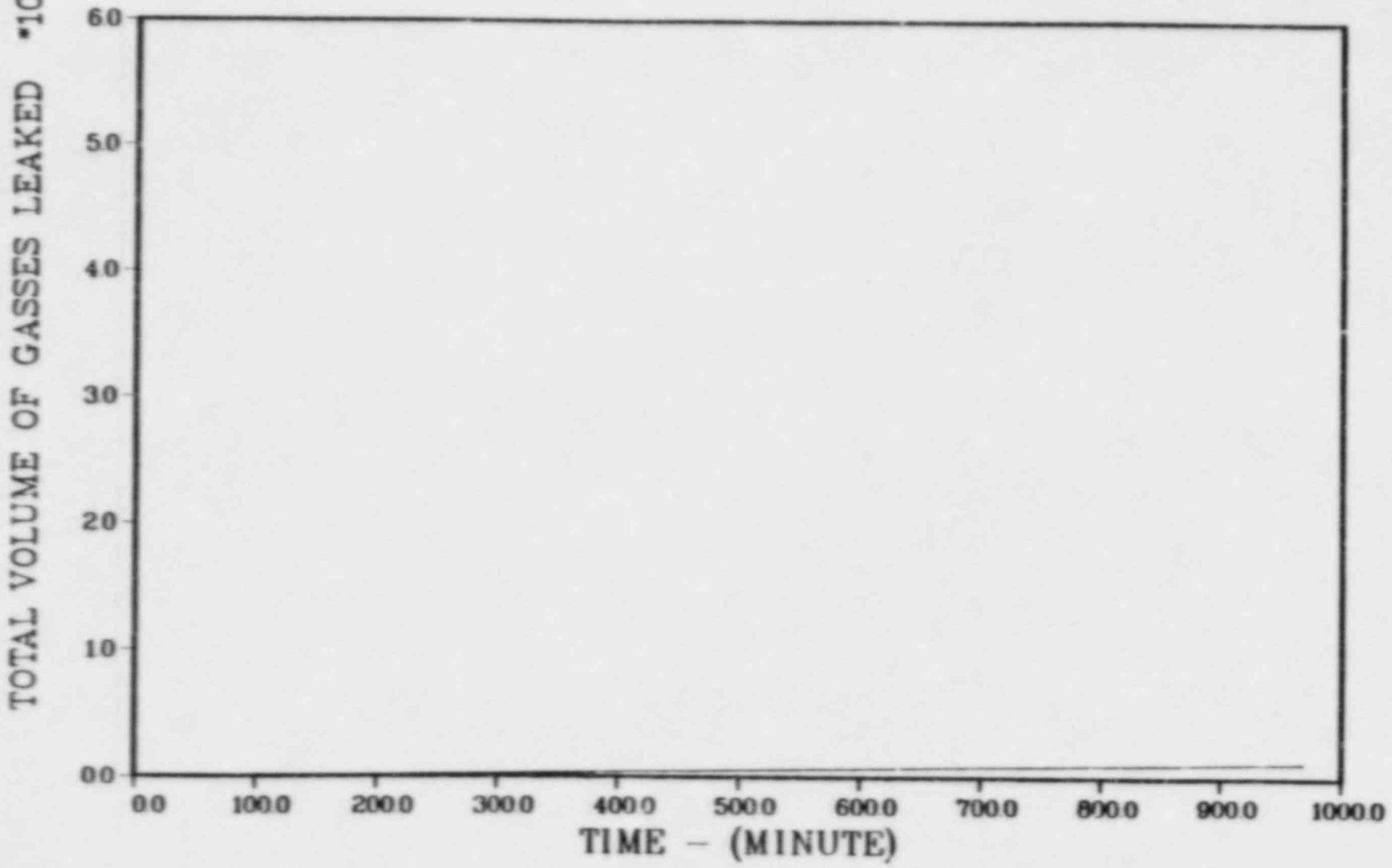

FIGURE 5. TOTAL VOLUME OF LEAKED GASES (MEDIUM LEAK)

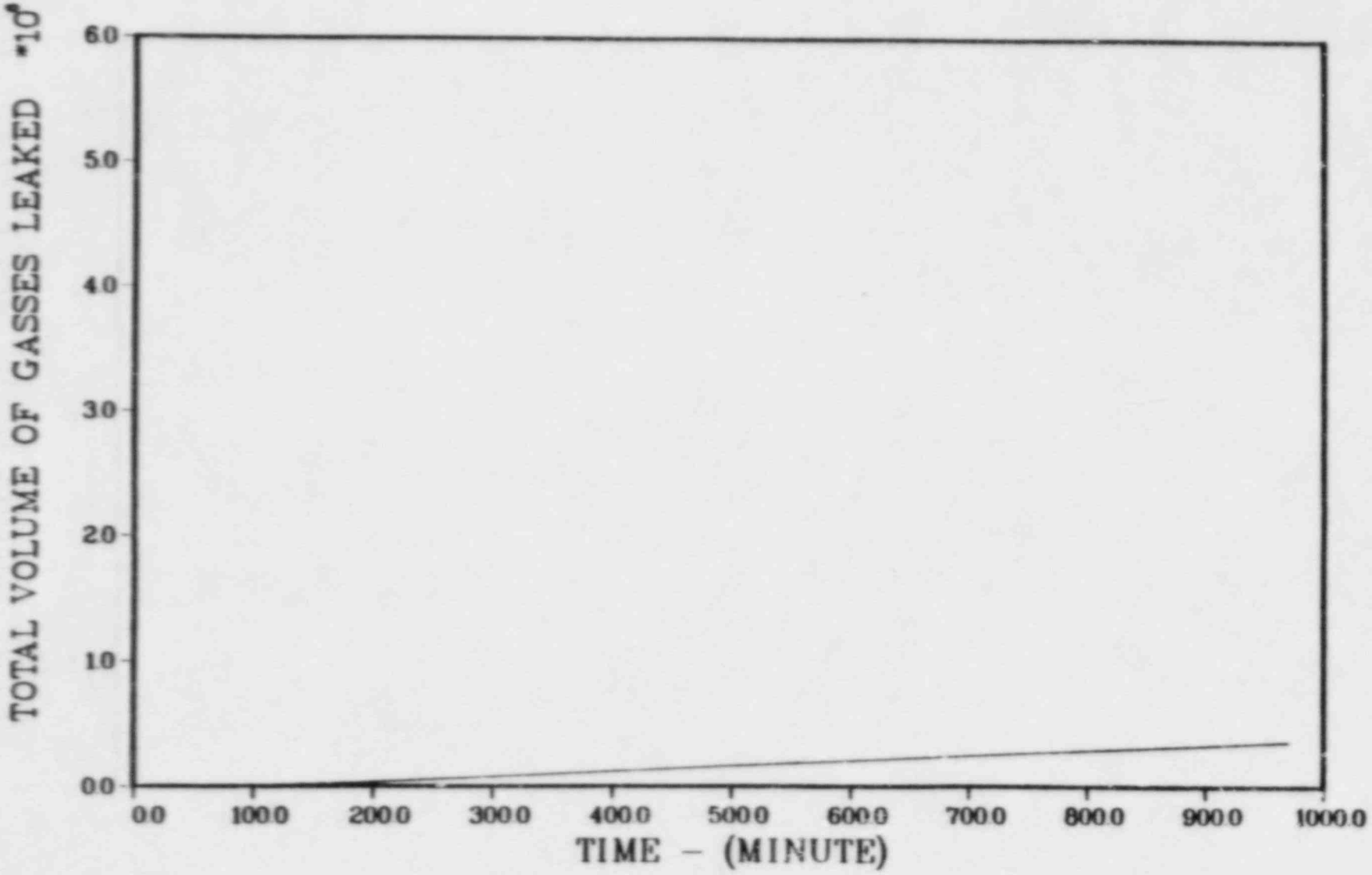

FIGURE 6. TOTAL VOLUME OF LEAKED GASES (HIGH LEAK)

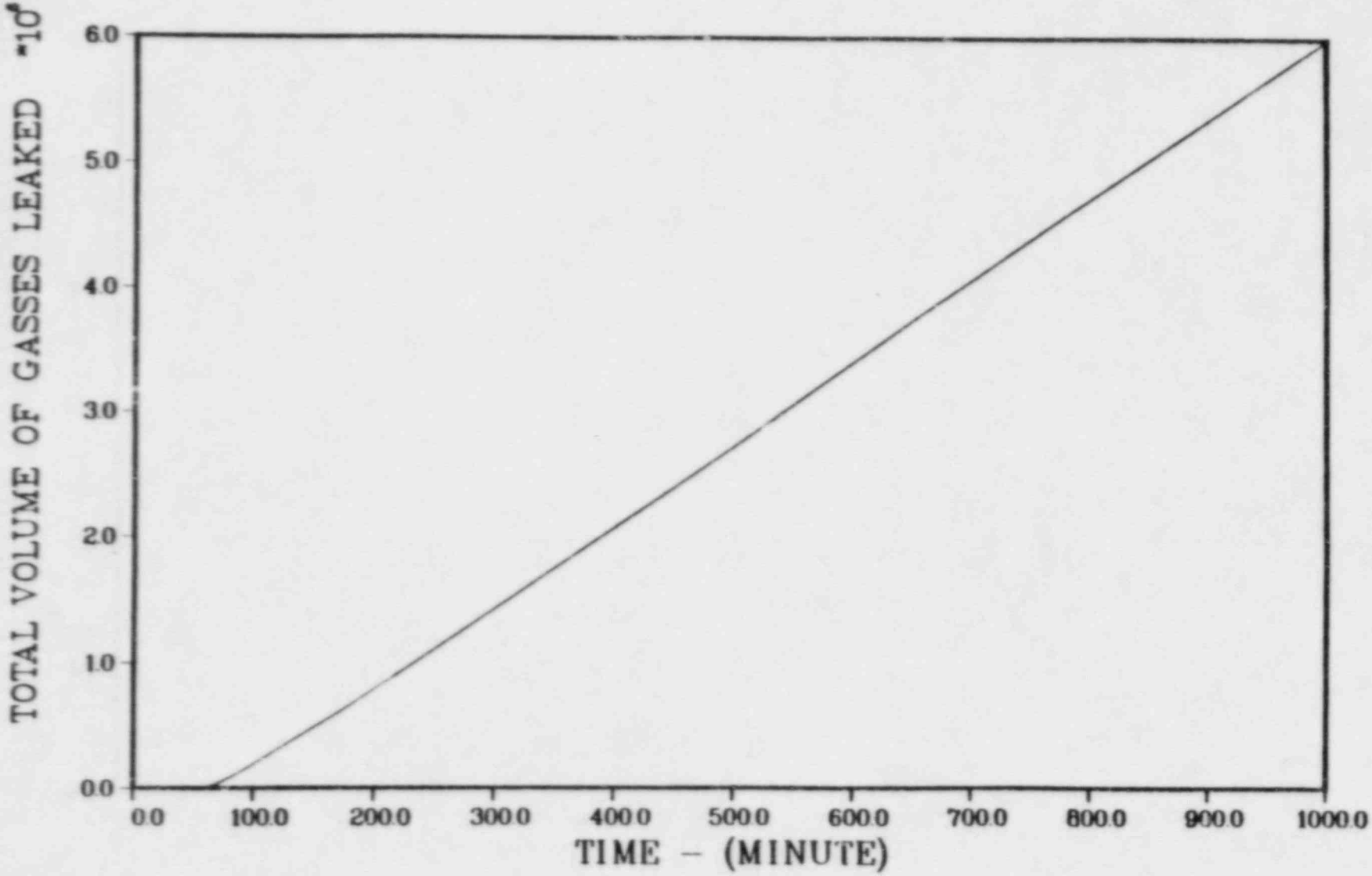

FIGURE 7. TOTAL VOLUME OF LEAKED GASES (ISOLATION FAILURE)

The results of the assessment of fission product releases to the environment for the various cases considered are summarized in Table 3. The effect of containment failure mode assumptions is most dramatic for tellurium, where the predicted release is seen to be 22 percent for the case of containment isolation failure. This is because much of the tellurium release from the fuel is predicted to take place directly to the containment after vessel head failure. The effect of increasing leak rate on the predicted release of CsI and CsOH is not as dramatic, though still noticeable.

Surry -- Subatmospheric PWR

The analyses for the Surry subatmospheric containment PWR were again based on the TMLB' accident sequence. The specific conditions and assumptions utilized in the analyses were very similar to those of the TMLB'-6 case treated in Volume V of BMI-2104 in which the containment was assumed to fail as a result of the steam spike from the interaction of the core debris with water in the reactor cavity following vessel head failure.

Two containment failure modes were explicitly considered for the Surry design in this study. The first corresponds to the high leak case as postulated by the CPWG. The leak area as a function of containment pressure as shown in Table 4 was used for this case. The second case was an assumed containment isolation failure with an opening equivalent to 6 inches in diameter.

Table 5 gives the accident event times for the Surry TMLB'-6 sequence as it was evaluated in Volume V of BMI-2104; as noted previously, in the latter it was assumed that containment failure was caused by the steam spike from the interaction of the core debris with water in the reactor cavity following vessel failure. Figures 8 and 9 give the containment pressure and temperature responses for this sequence; Figure 10 shows the total volume of gases leaked as a function of time corresponding to the assumed large opening at containment failure.

For the analysis of the alternate containment failure modes, the response of the primary system was found to be essentially the same

TABLE 3. LOCATIONAL DISTRIBUTION OF FISSION PRODUCTS FOR VARIOUS CONTAINMENT FAILURES MODES OF THE ZION PLANT (TMLB')

Unit: Fraction of Core Inventory

	RCS	Containment	Environment
		BMI-2104 (Normal Leak)	
CsI	0.98	2.5×10^{-2}	1.9×10^{-6}
CsOH	0.98	2.5×10^{-2}	1.9×10^{-6}
Te	0.29	0.63	7.8×10^{-5}
		Medium Leak	
CsI	0.98	2.5×10^{-2}	7.1×10^{-5}
CsOH	0.98	2.5×10^{-2}	7.2×10^{-5}
Te	0.29	0.63	5.5×10^{-3}
		High Leak	
CsI	0.98	2.5×10^{-2}	9.0×10^{-5}
CsOH	0.98	2.5×10^{-2}	9.1×10^{-5}
Te	0.29	0.62	1.6×10^{-2}
		Isolation Failure	
CsI	0.98	1.8×10^{-2}	7.0×10^{-3}
CsOH	0.98	1.8×10^{-2}	7.1×10^{-3}
Te	0.29	0.42	2.2×10^{-1}

TABLE 4. SURRY LEAKAGE MODEL

Pressure, psia	Leak Area, in^2		
	Low	Medium	High
9.9	0.10	0.50	1.00
32.9	0.10	0.60	1.50
56.9	0.10	0.60	1.80
105.3	0.10	2.10	11.00

TABLE 5. ACCIDENT EVENT TIMES

Event	Time, minutes
Steam generator dry	67.5
Core uncover	95.5
Start melt	118.3
Core slump	146.3
Core collapse	148.0
Bottom head fail	152.8
Containment fail	152.9
Reactor cavity dry	177.2
Start concrete attack	254.2
End calculation	1073.4

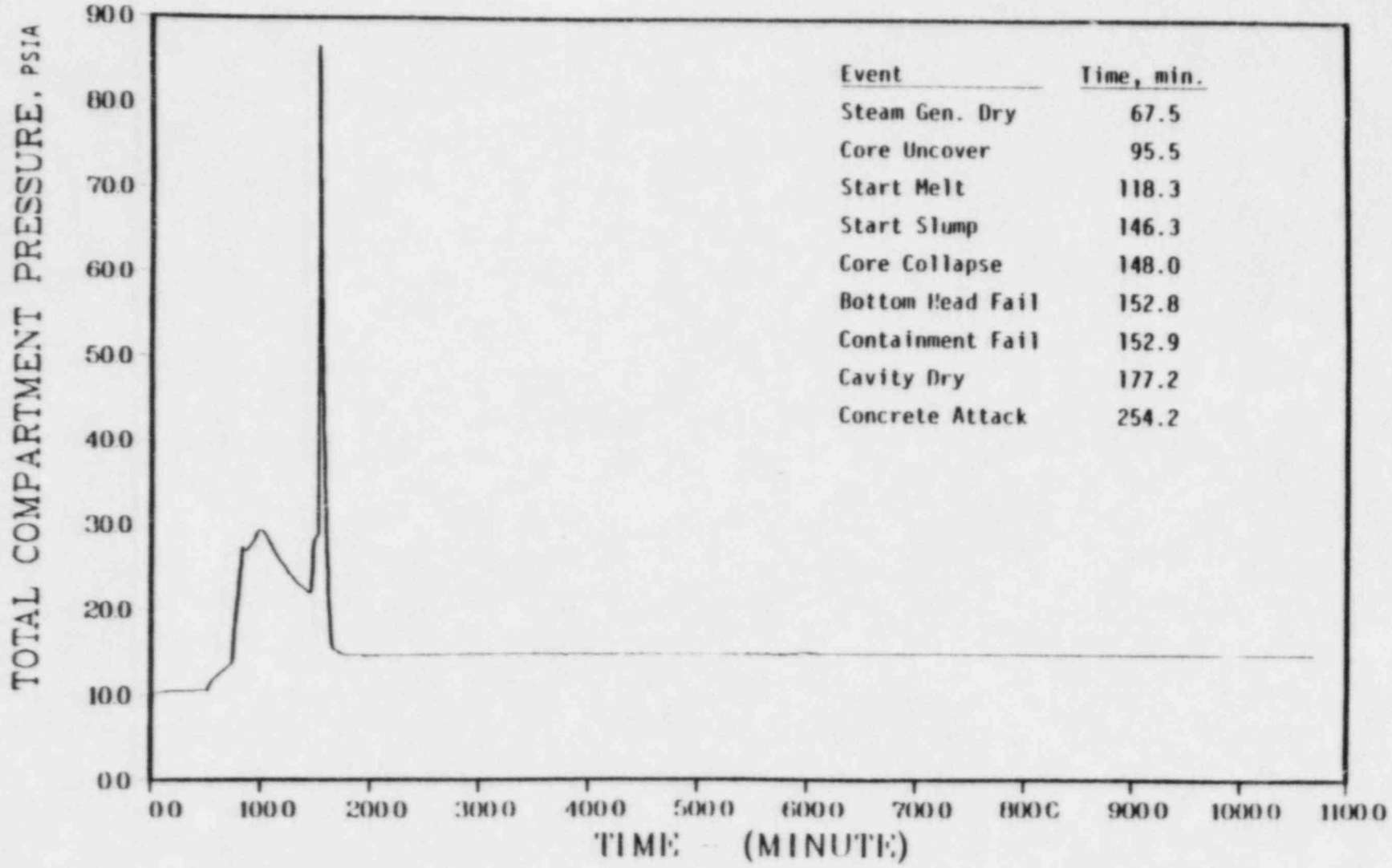

FIGURE 8. CONTAINMENT PRESSURE RESPONSE FOR SURRY TMLB'-δ SEQUENCE

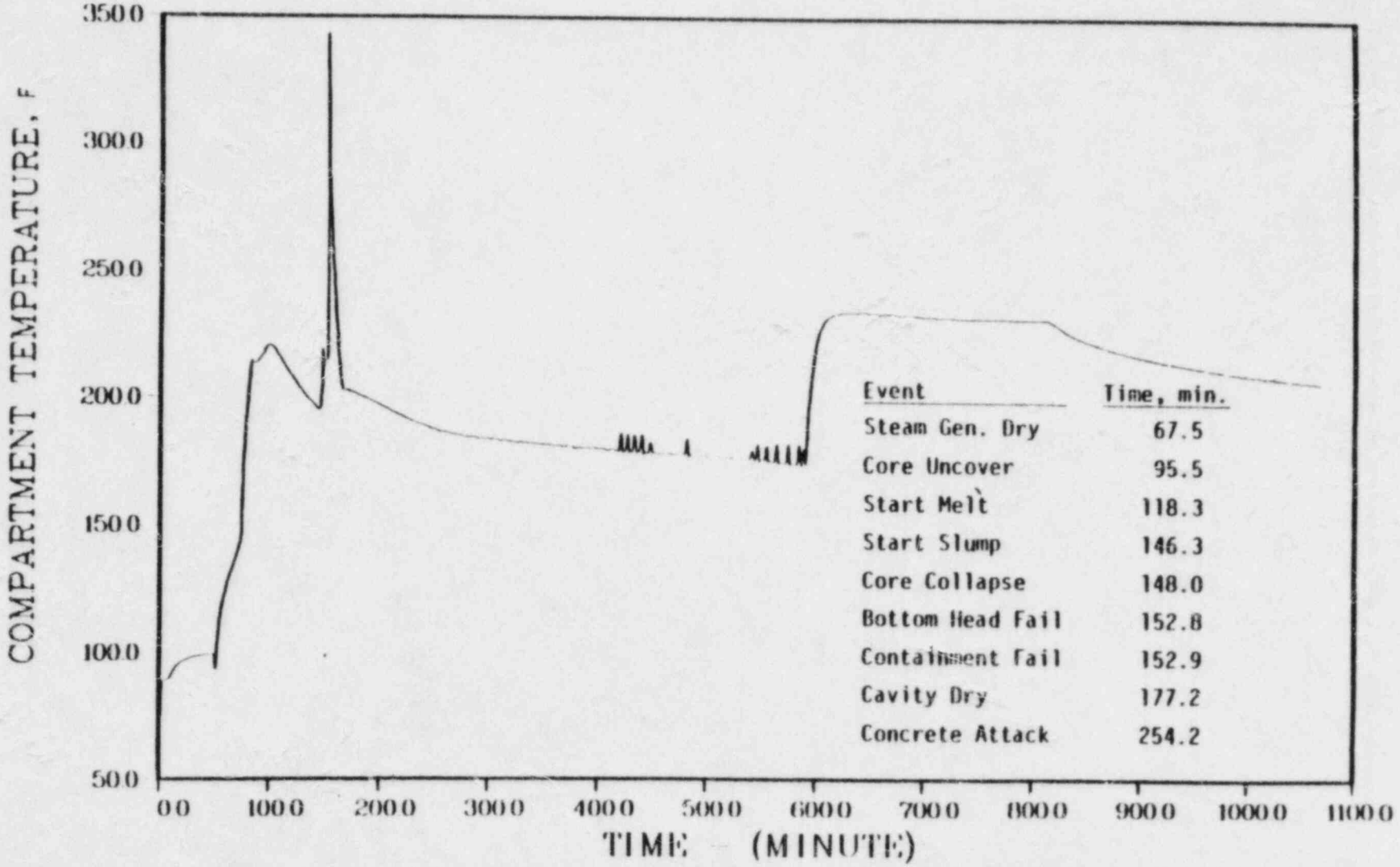

FIGURE 9. CONTAINMENT TEMPERATURE RESPONSE FOR SURRY TMLB'-6 SEQUENCE

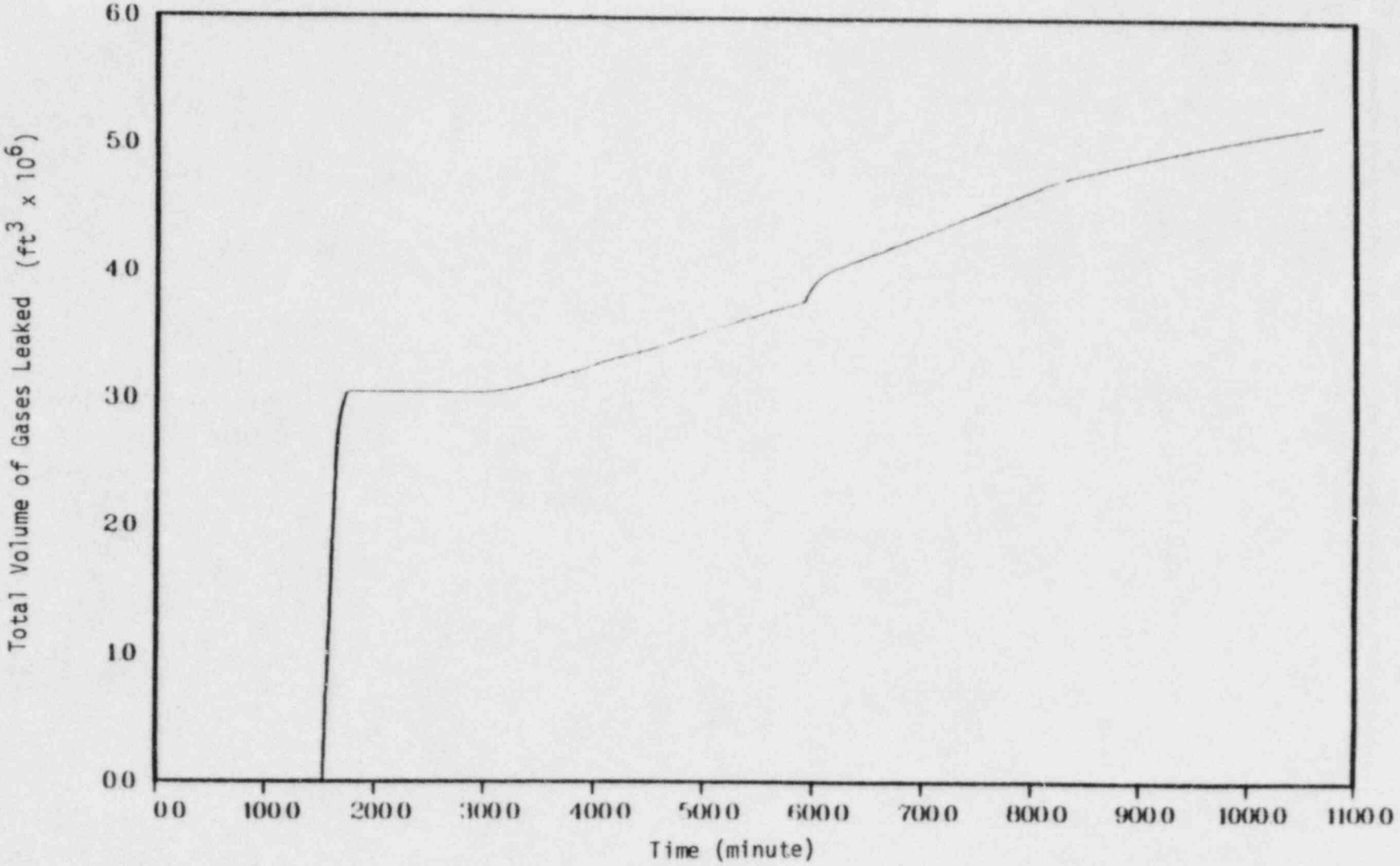

FIGURE 10. TOTAL VOLUME OF GASES LEAKED FOR SURRY TMLB-δ SEQUENCE

as in the earlier analyses; thus the previously evaluated primary system fission product releases were used. The containment was modeled as a single compartment identical to the approach previously used for this sequence. It is, of course, possible that the leakages would be initially into secondary containment structures rather than directly to the environment. The effects of secondary containment structures have not been addressed in the present study since their possible effect can be inferred from the results of other sequences reported in BMI-2104. The high leakage model as defined in Table 4 was used in the MARCH containment analysis; the resulting containment pressure and temperature responses are illustrated in Figures 11 and 12. It should be noted that the containment pressure did not reach the level corresponding to the last entry of Table 4. The relatively small leak areas associated with the pressures that are predicted in this case have a minimal effect on the peak containment pressure predicted. Figure 13 gives the containment leak rate as a function of time, and Figure 14 gives the integrated leakage for this model. The changes in the leak rate as the pressure rises are clearly seen in Figure 13.

The failure of the containment to isolate was modeled as an opening 6 inches in diameter, existing at the start of the accident. The containment was again modeled as a single compartment without consideration of the possible effects of secondary containment structures. For the cases of isolation failure it is likely that the opening in the primary containment would be to some portion of the secondary containment; the assumption of direct release to the environment is a simplification in the analysis. The containment pressure and temperature responses assuming containment isolation failure are illustrated in Figures 15 and 16. The corresponding leak rates and total leakage are given in Figures 17 and 18. It is obvious that the leakages associated with the assumed isolation failure are substantially higher than those for the "high leak" case. It should further be noted that the total leakage for the BMI-2104 case is even higher than that for the assumed isolation failure when Figures 10 and 18 are compared.

Table 6 shows the results of the transport calculation for fission products under the conditions described above. It is seen that

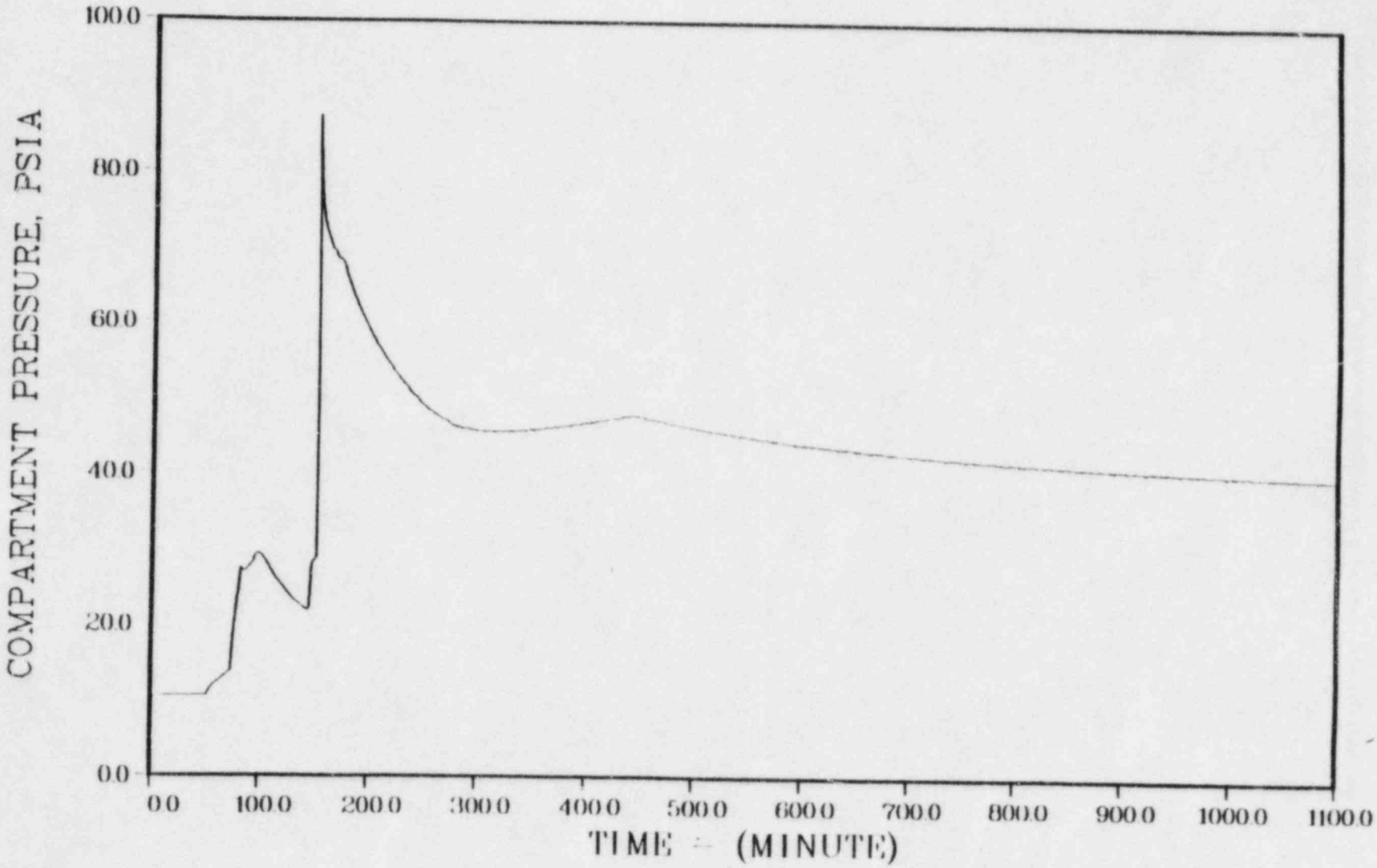

FIGURE 11. CONTAINMENT PRESSURE RESPONSE FOR SURRY TMLB WITH HIGH LEAKAGE

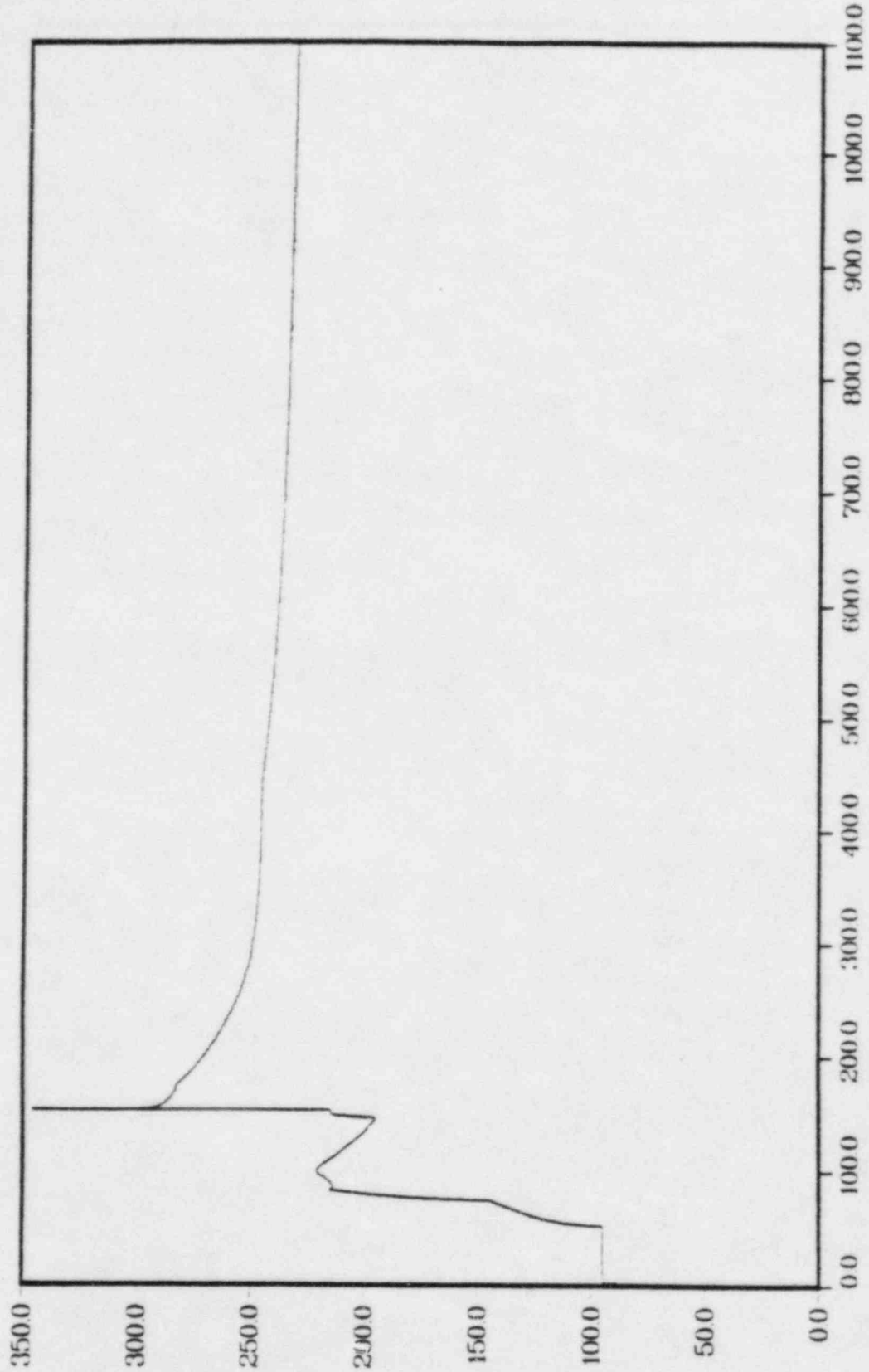

FIGURE 12. CONTAINMENT TEMPERATURE RESPONSE FOR SURRY TMLB WITH HIGH LEAKAGE

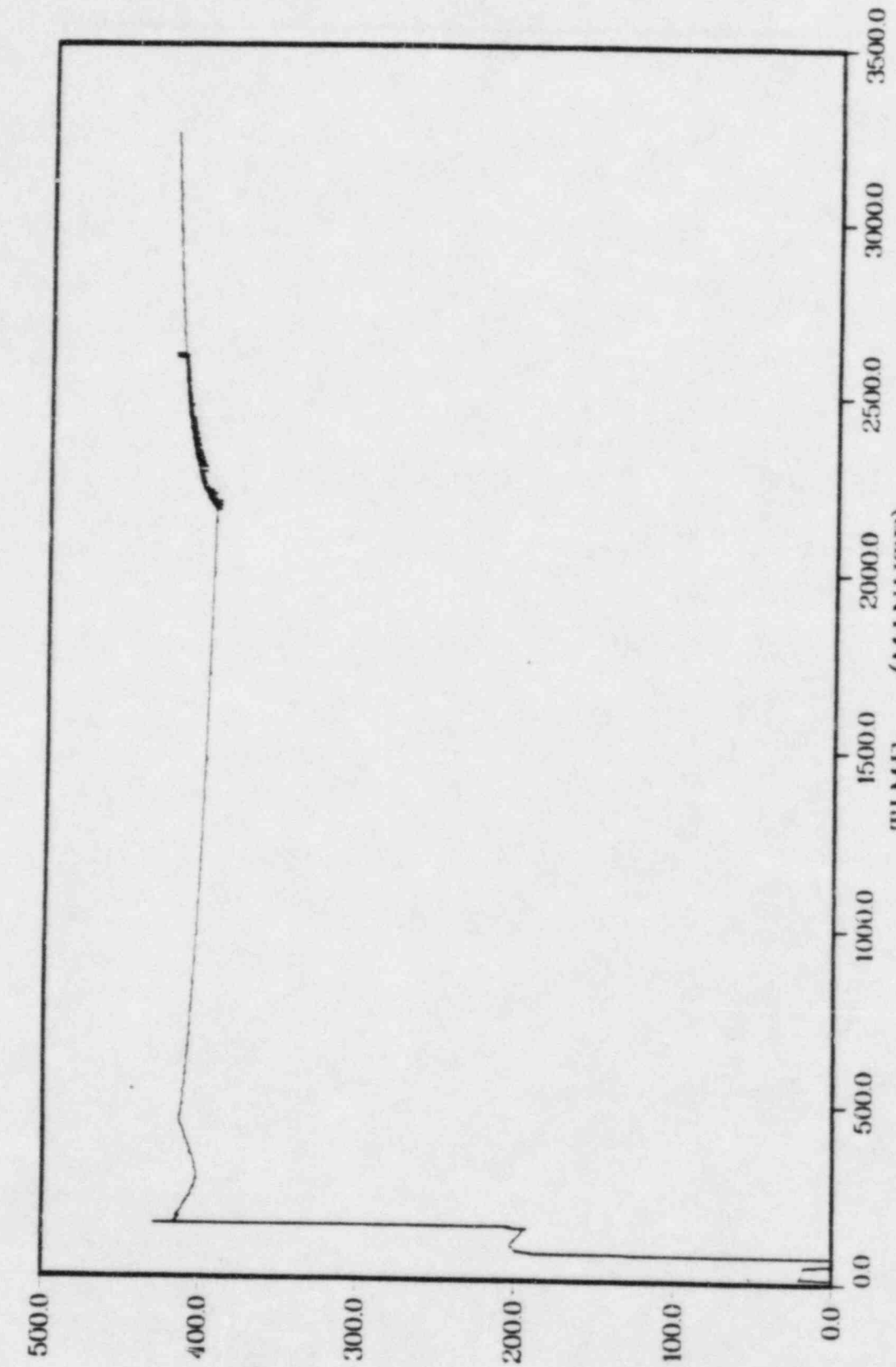

FIGURE 13. CONTAINMENT LEAK RATE FOR SURRY TMLB WITH HIGH LEAKAGE

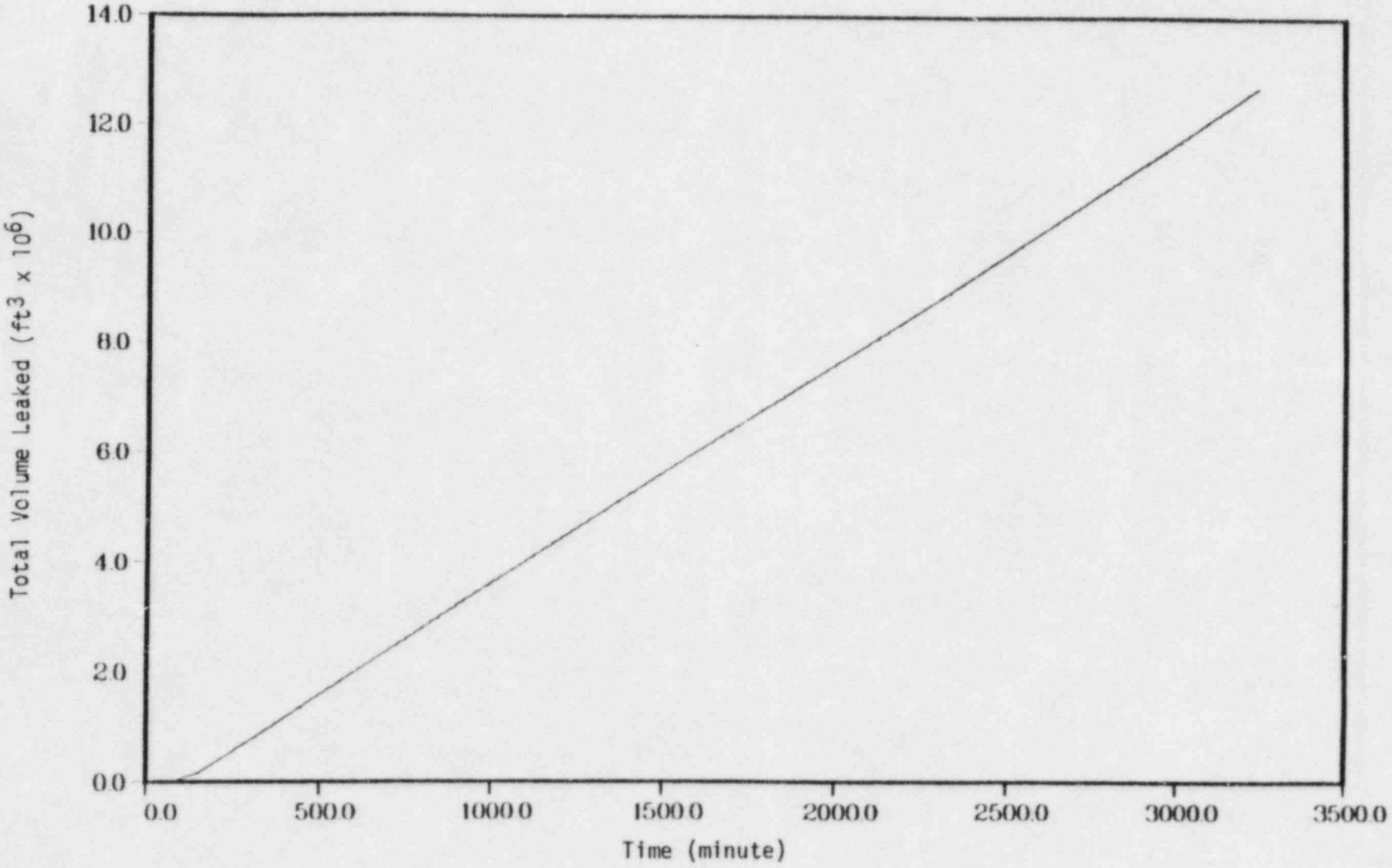

FIGURE 14. TOTAL GAS LEAKAGE FOR SURRY TMLB WITH HIGH LEAKAGE

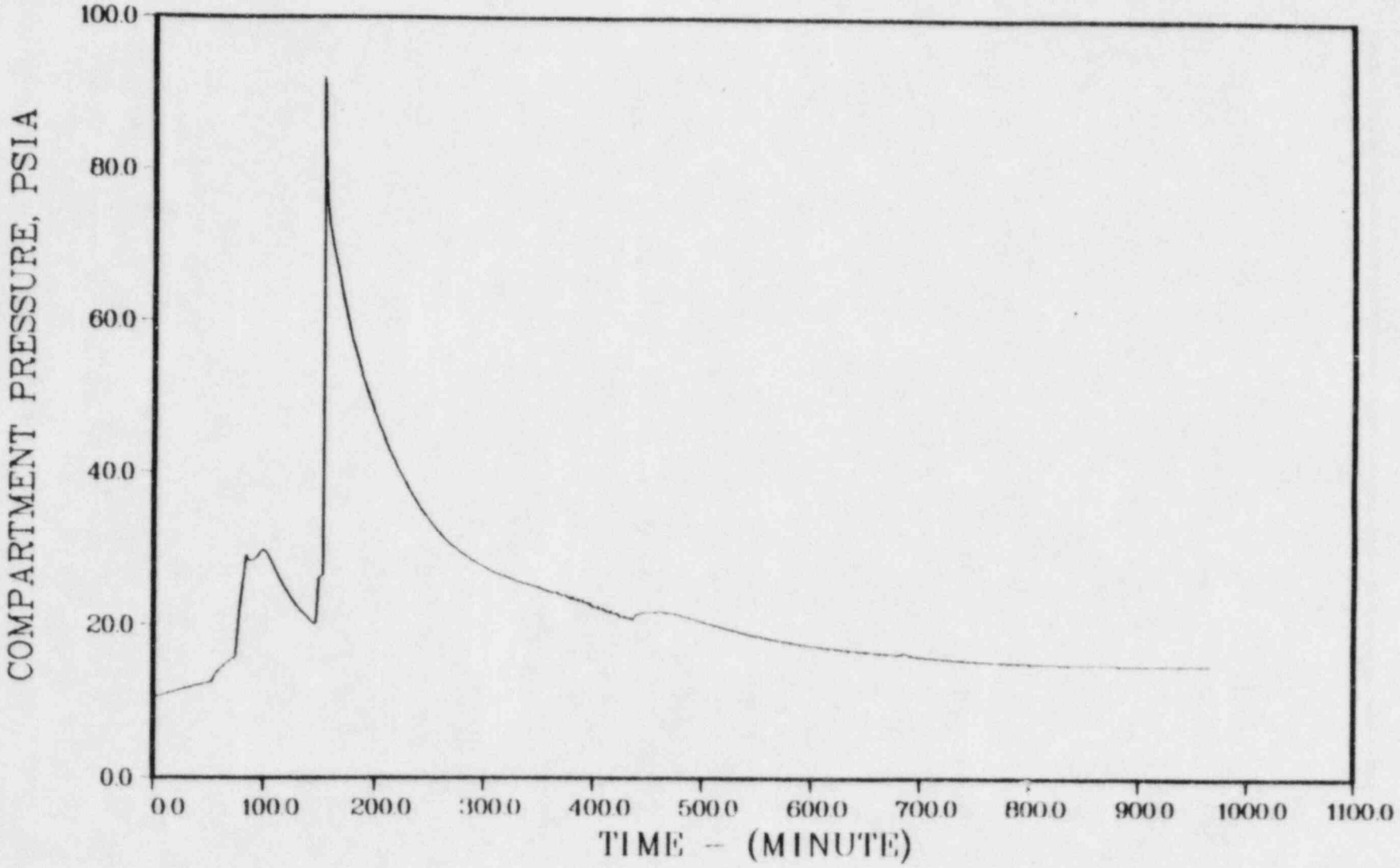

FIGURE 15. CONTAINMENT PRESSURE RESPONSE FOR SURRY TMLB WITH ISOLATION FAILURE

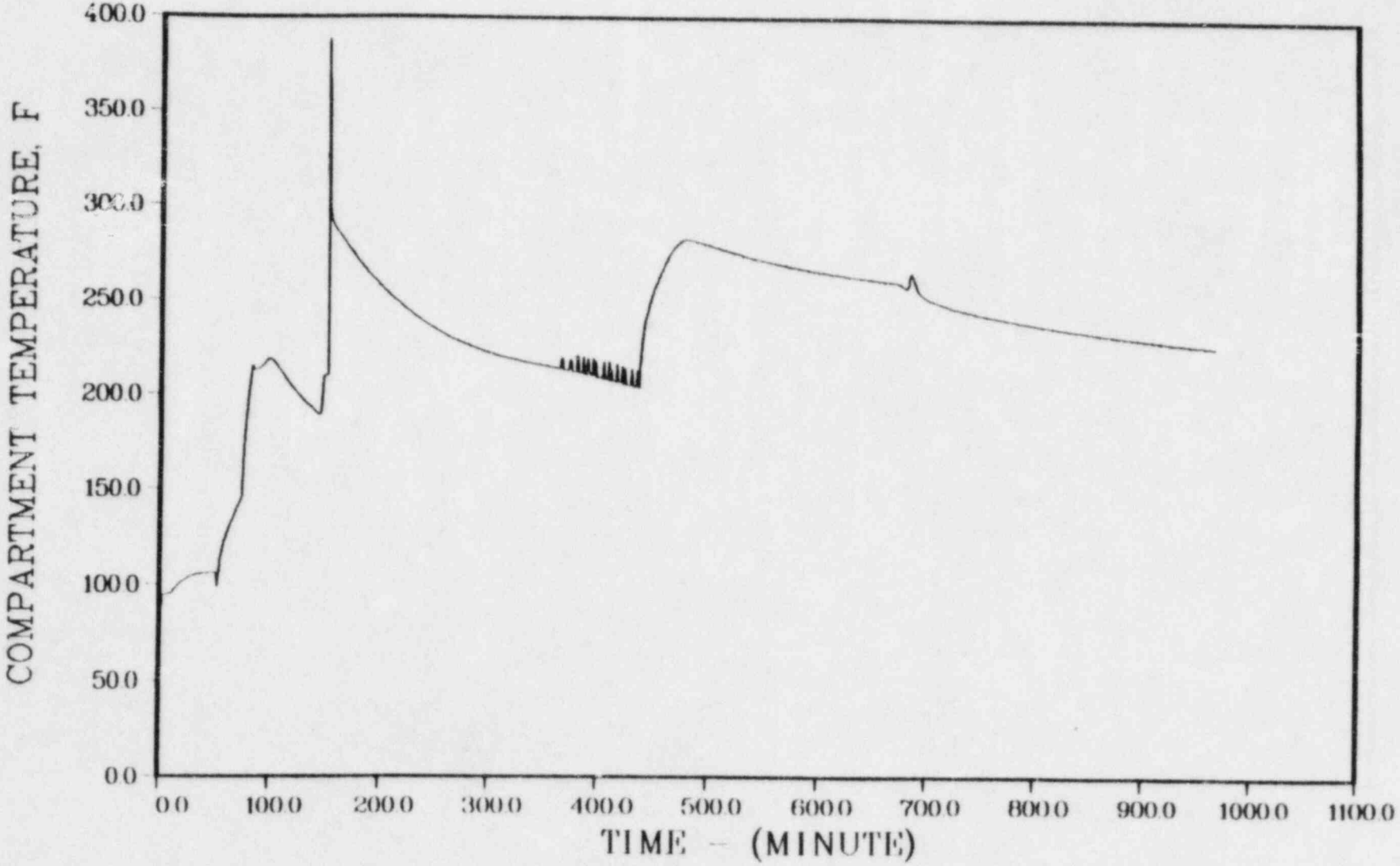

FIGURE 16. CONTAINMENT TEMPERATURE RESPONSE FOR SURRY TMLB WITH ISOLATION FAILURE

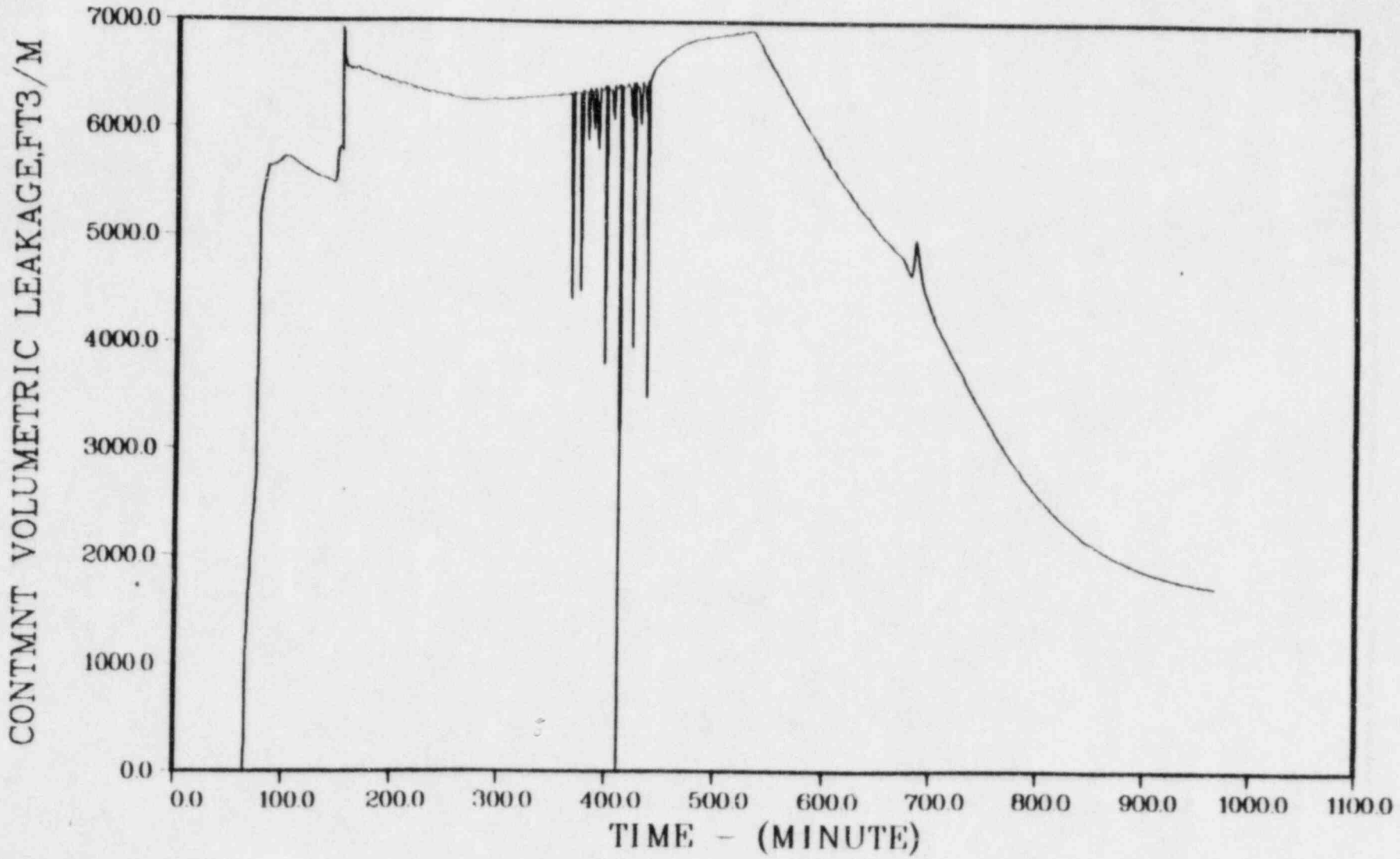

FIGURE 17. CONTAINMENT LEAK RATE FOR SURRY TMLB WITH ISOLATION FAILURE

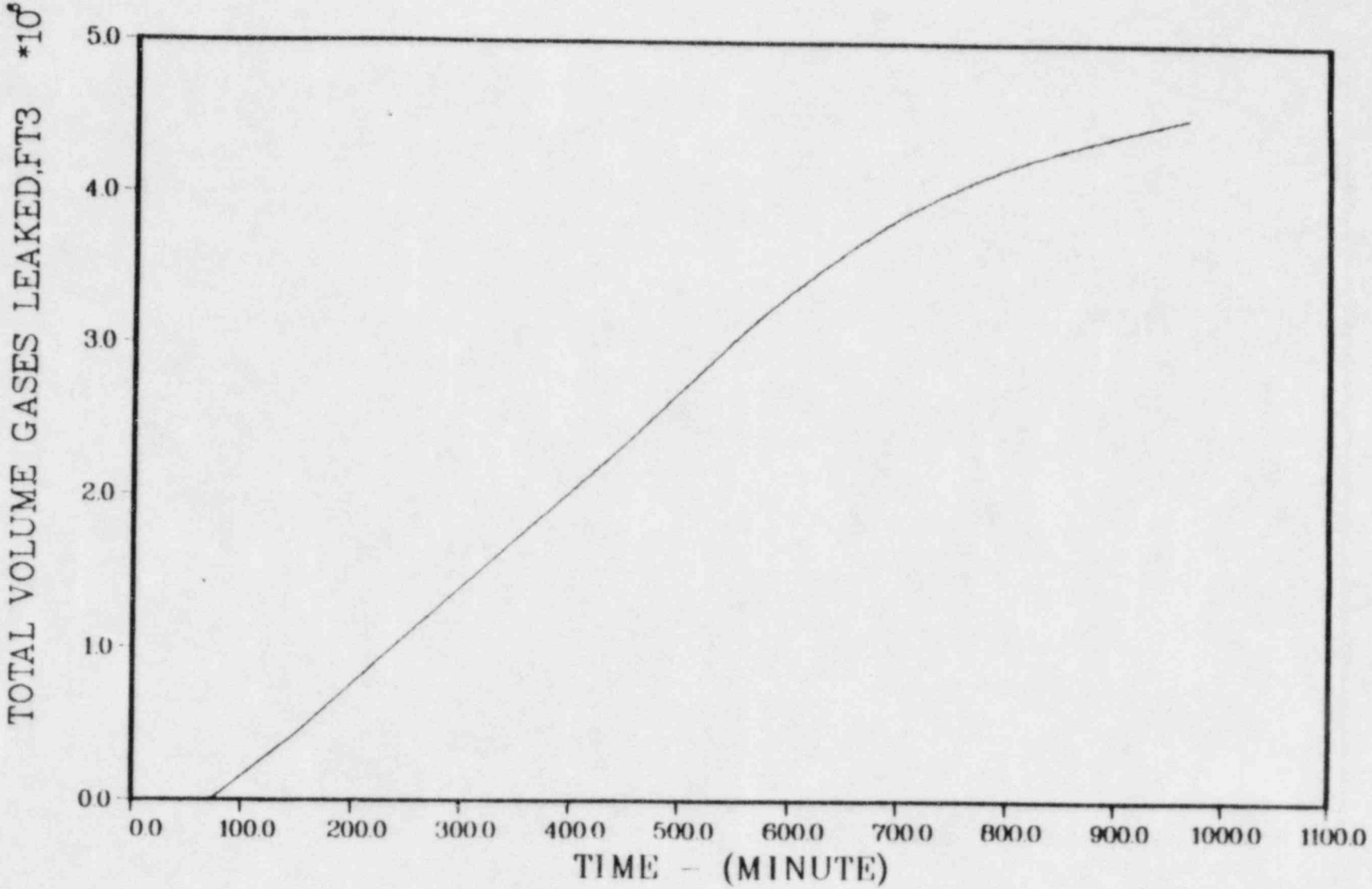

FIGURE 18. TOTAL LEAKAGE FOR SURRY TMLB WITH ISOLATION FAILURE

TABLE 6. LOCATIONAL DISTRIBUTION OF FISSION PRODUCTS FOR VARIOUS CONTAINMENT FAILURE MODES OF THE SURRY PLANT (TMLB')

Unit: Fraction of core inventory

Species	RCS	Containment	Environment
		BMI-2104	
CsI	0.85	0.11	4.6×10^{-2}
CsOH	0.86	0.10	3.9×10^{-2}
Te	0.30	0.59*	1.1×10^{-1}
		High Leak	
CsI	0.85	0.15	1.9×10^{-3}
CsOH	0.86	0.14	1.1×10^{-3}
Te	0.30	0.69*	1.2×10^{-2}
		Isolation Failure	
CsI	0.85	0.13	2.2×10^{-2}
CsOH	0.86	0.13	1.3×10^{-2}
Te	0.30	0.50*	1.1×10^{-1}

*The number includes a fraction of 0.43 for Te not released from the core melt.

the fraction of core inventory that is captured in the containment is the highest in the "high leak" case primarily due to the relatively small leakage rates. As a result, the case registers the lowest fractions that are released to the environment. It is interesting to note that among the cases investigated here, the BMI-2104 case yields the largest release fraction suggesting that containment failure modes can affect the release of fission products in a rather subtle manner. The implication is that the volume of the gases leaked depends upon the containment pressure and the hole size. A high pressure spike, such as the one seen in Figure 8, tends to create a large hole size causing the containment to depressurize rapidly. Another consideration is, of course, the timing of the fission product source with respect to the leakage rate. For example, Te which tends to be released to the containment over a relatively longer time is affected to a lesser degree by early leakage characteristics.

Sequoyah -- Ice Condenser PWR

For the ice condenser PWR, the alternate containment failure mode considered was failure of the containment to isolate at the start of the accident. The isolation failure was modeled as a 6-inch diameter opening in the lower compartment of the ice condenser containment communicating with the secondary containment. The secondary containment was assumed to have a free volume of 1,000,000 cubic feet and a representative set of structures. The secondary containment was assumed to have a sufficiently large opening to permit leakage of the gases and vapors released to it without appreciable pressure buildup. The effect of the secondary containment was not considered previously in the BMI-2104 analyses for this containment design.

The accident sequence selected for this study was again the TMLB accident previously considered. In the BMI-2104 analyses for this sequence, it was found that the containment integrity could be threatened by an early hydrogen burn as well as by long-term overpressurization. Table 7 presents the accident event times for the two variations of this sequence as they were derived in BMI-2104. Figures 19 and 20 illustrate

TABLE 7. ACCIDENT EVENT TIMES

Event	Time, minutes
	Sequoyah TMLB'-Y
Steam Generator Dry	62.0
Core Uncover	97.8
Start Melt	121.5
Start Slump	143.5
Core Collapse	145.0
Vessel Head Dry	149.2
Bottom Head Fail	157.8
Containment Fail	157.8
Concrete Attack	158.9
Ice Melt Complete	428.5
End Calculation	761.2
	Sequoyah TMLB'-δ
Steam Generator Dry	62.0
Core Uncover	97.8
Start Melt	121.5
Start Slump	143.5
Core Collapse	145.0
Vessel Head Dry	149.2
Bottom Head Fail	157.8
Concrete Attack	161.5
Containment Fail	552.5
Ice Melt Complete	556.0
End Calculation	761.6

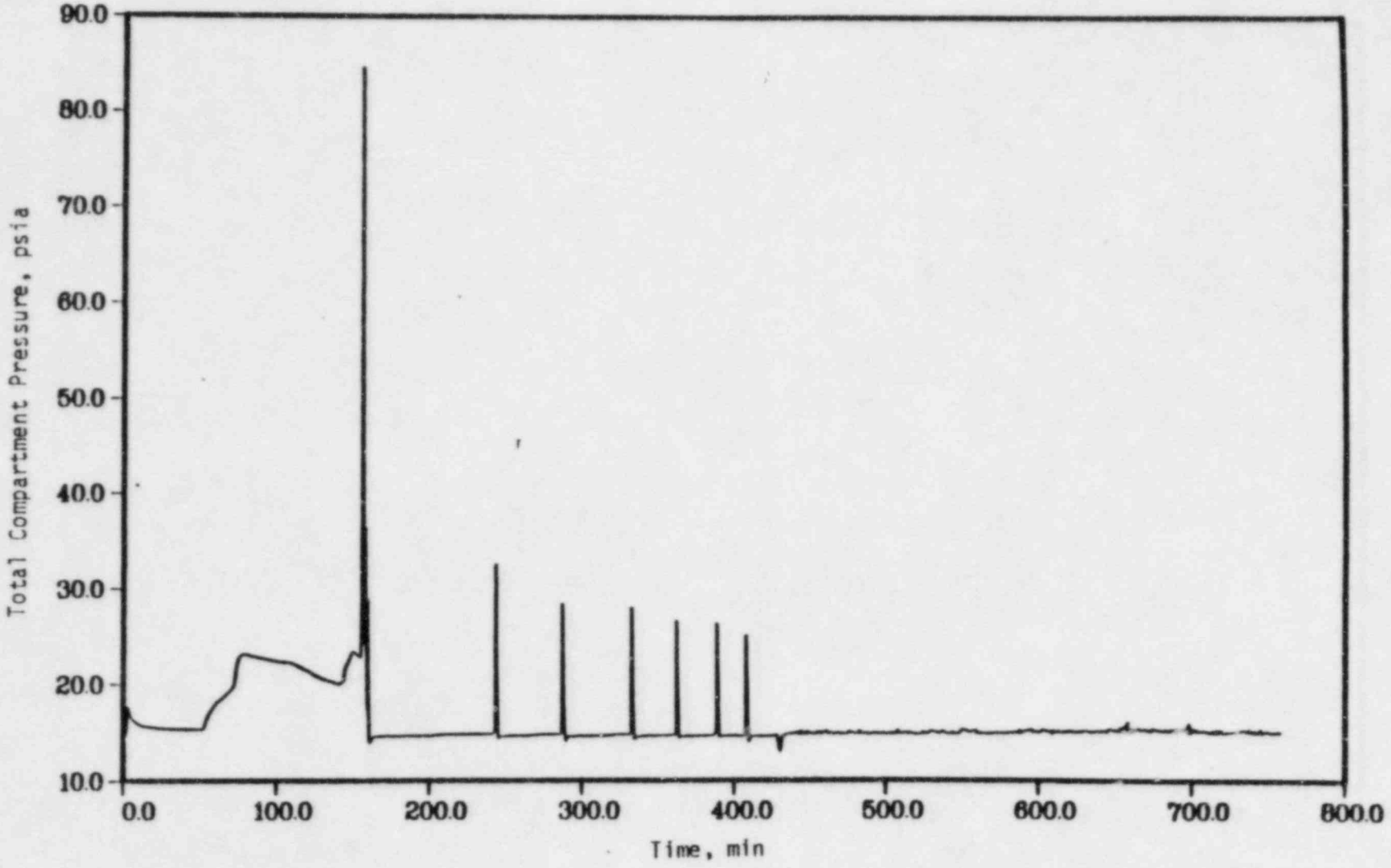

FIGURE 19. CONTAINMENT PRESSURE FOR SEQUOYAH TMLB'-γ SEQUENCE

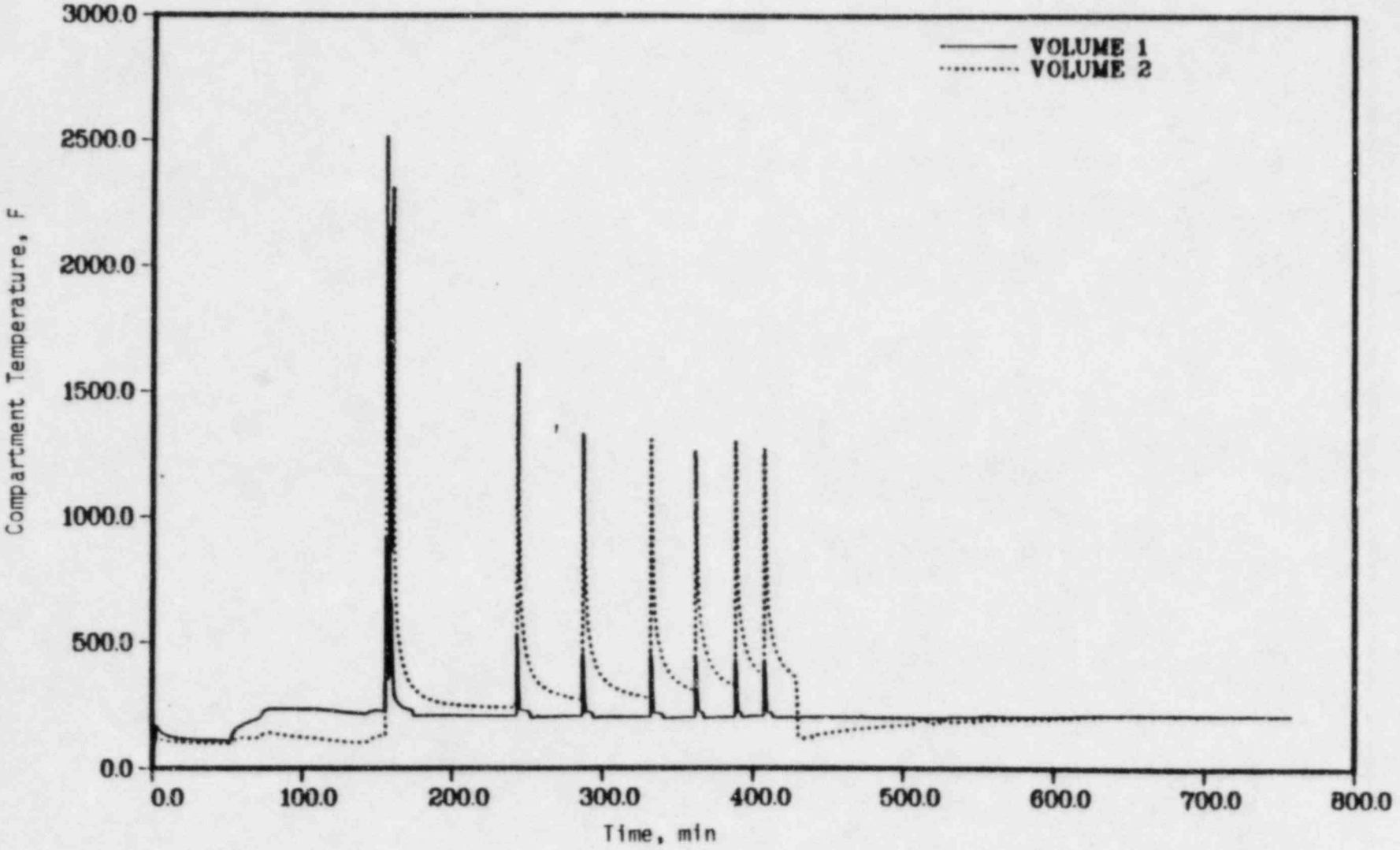

FIGURE 20. CONTAINMENT TEMPERATURE RESPONSE FOR SEQUOYAH TMLB'-γ SEQUENCE

the containment pressure and temperature responses for the case of early containment failure due to hydrogen burning as presented in BMI-2104. Figures 21 and 22 show the corresponding responses for the long-term overpressure case.

Since the primary system response for the containment isolation case was substantially the same as previously calculated, the fission product release from the primary system to the containment was taken from the earlier analyses and only the containment transport and leakage were reevaluated.

Figures 23 and 24 show the containment pressure and temperature responses calculated for the containment isolation failure case. It is interesting to note that the pressures resulting from hydrogen burns in the primary containment are still high enough that they could lead to containment failure, even in the presence of the preexisting leak. The burning is seen to take place in the upper compartment of the containment, consistent with earlier observations. The containment leak rate and total volume of gases leaked are illustrated in Figures 25 and 26. The leak rate is seen to be rather discontinuous in response to various transient events, such as hydrogen burns, whereas the integrated leakage is quite well behaved. These containment responses were used as the basis for the evaluation of fission product release to the environment. It should be noted that the assumption of the isolation failure in the lower compartment means that the airborne radioactivity leaking to the secondary containment does not have the benefit of scrubbing by the ice condenser.

Table 8 summarizes the results of the fission product transport calculations. It is seen that due to a large leakage rate and the ice condenser bypass, the isolation failure case yields much higher release fractions of fission products to the environment.

Grand Gulf -- Mark III BWR

For the BWR Mark III pressure suppression containment design, the failure to isolate at the start of the accident was selected as the characteristic noncatastrophic containment failure mode. The isolation failure was assumed to be in the outer containment with direct leakage

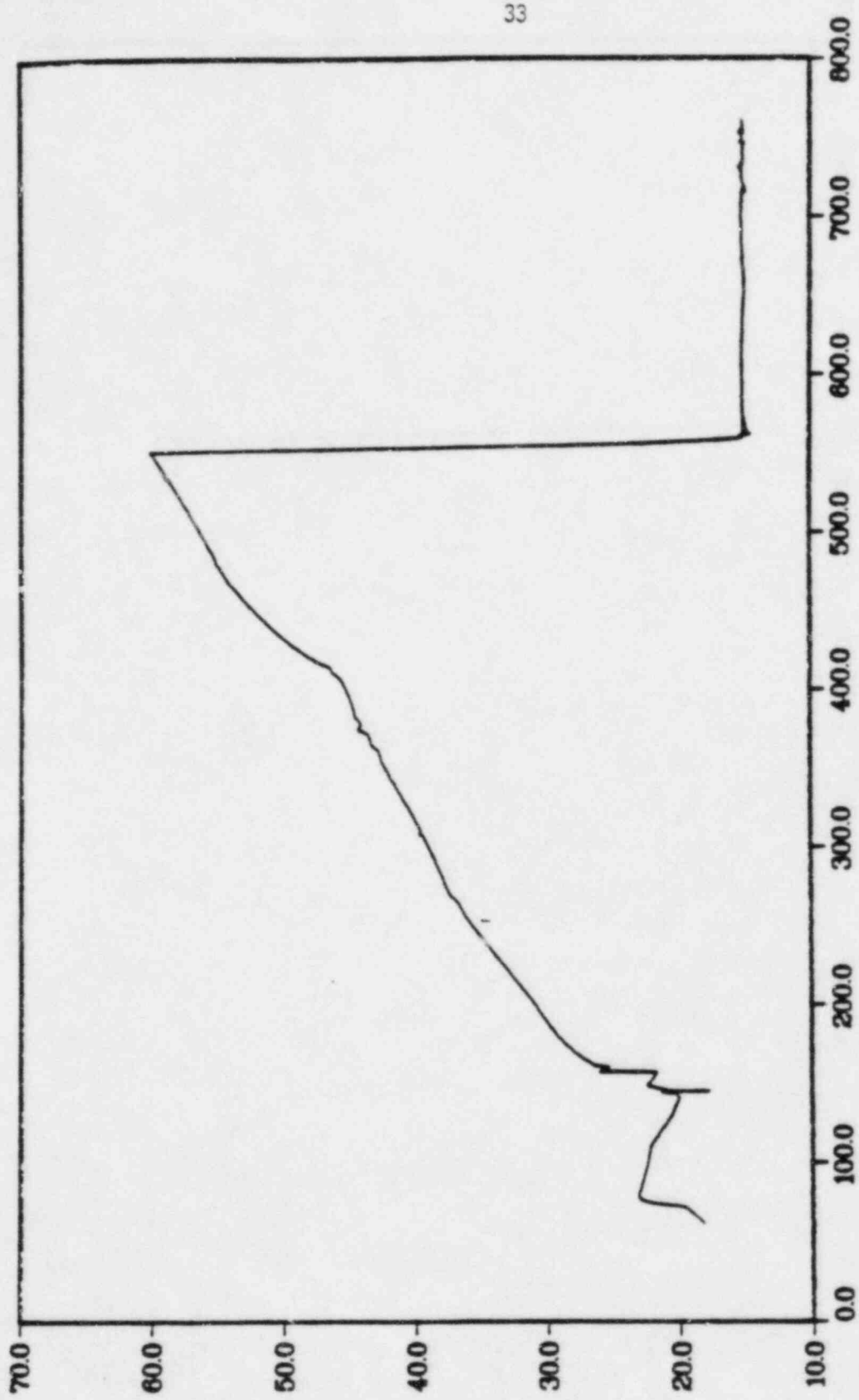

FIGURE 21. CONTAINMENT PRESSURE RESPONSE FOR SEQUOYAH TMLB'-δ SEQUENCE

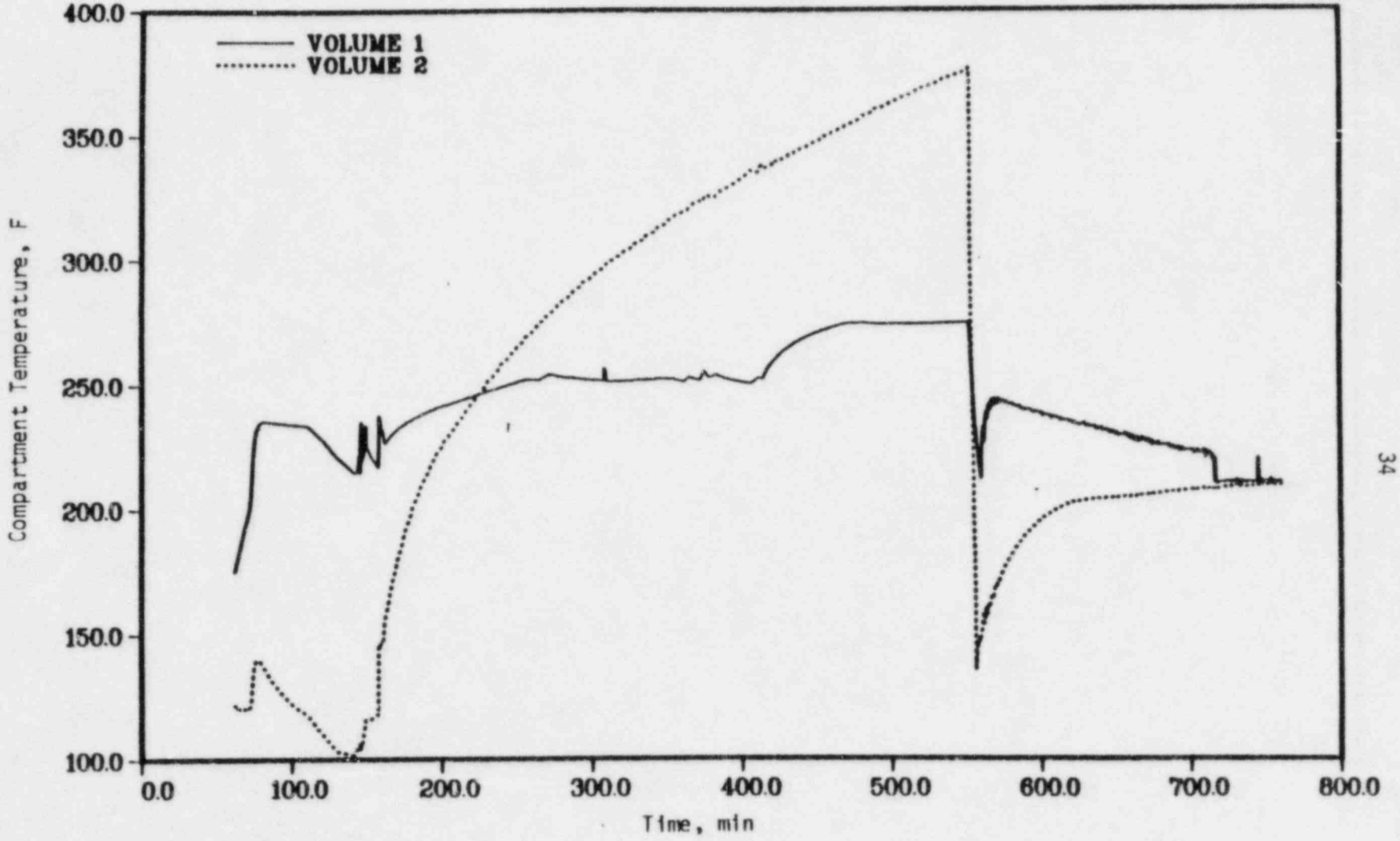

FIGURE 22. CONTAINMENT TEMPERATURE RESPONSE FOR SEQUOYAH TMLB'-δ SEQUENCE

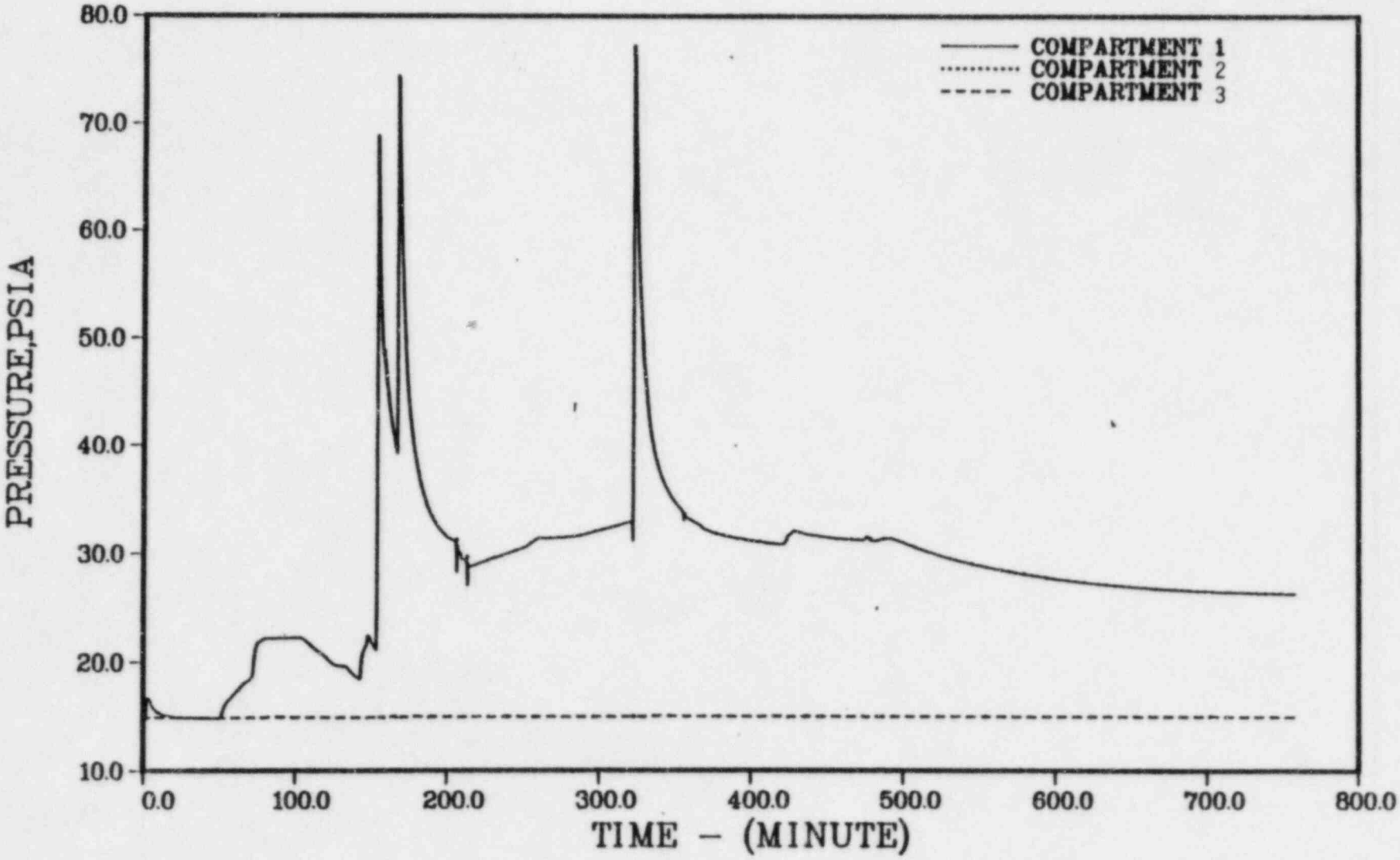

FIGURE 23. CONTAINMENT PRESSURE RESPONSE FOR SEQUOYAH TMLB WITH ISOLATION FAILURE

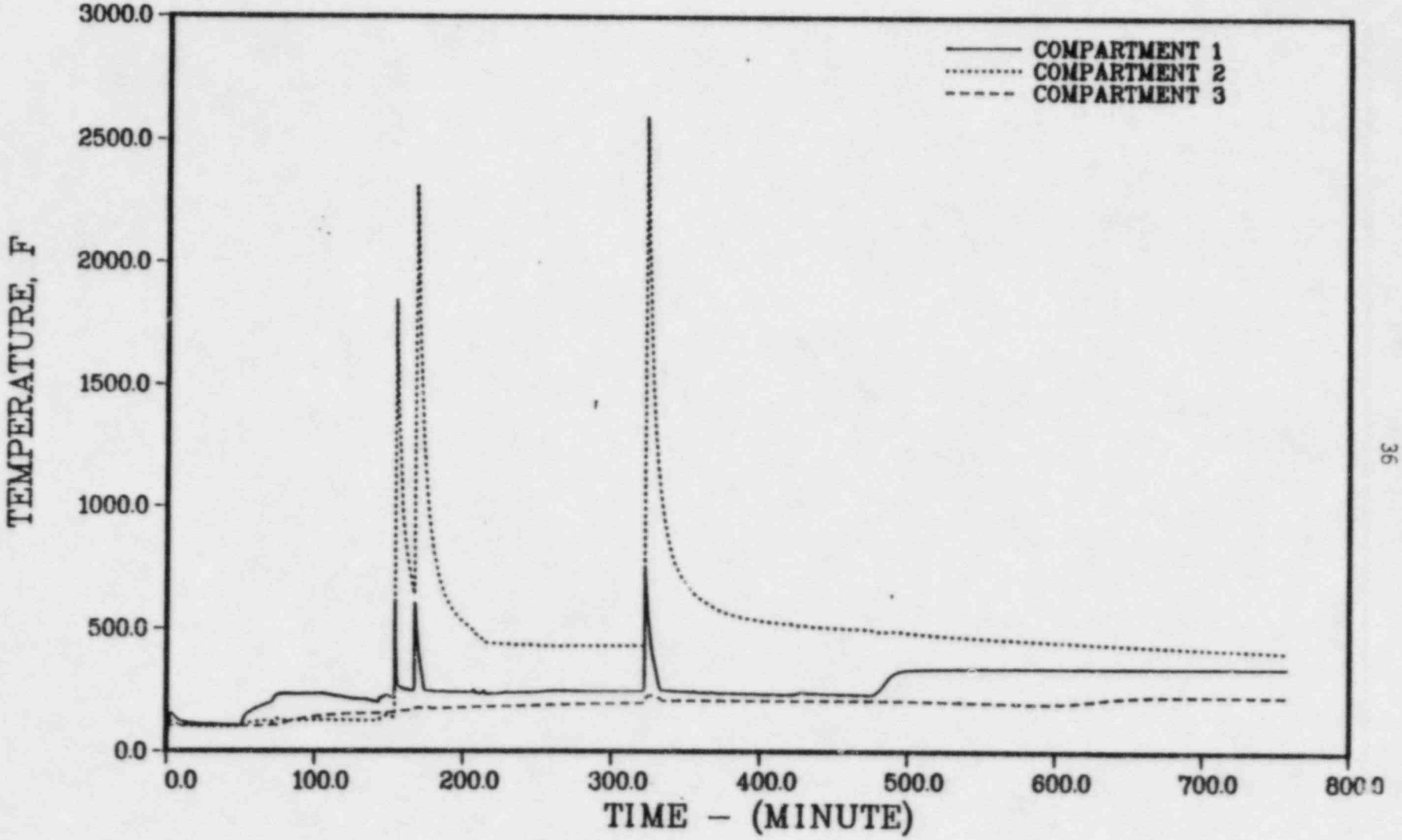

FIGURE 24. CONTAINMENT TEMPERATURE RESPONSE FOR SEQUOYAH TMLB WITH ISOLATION FAILURE

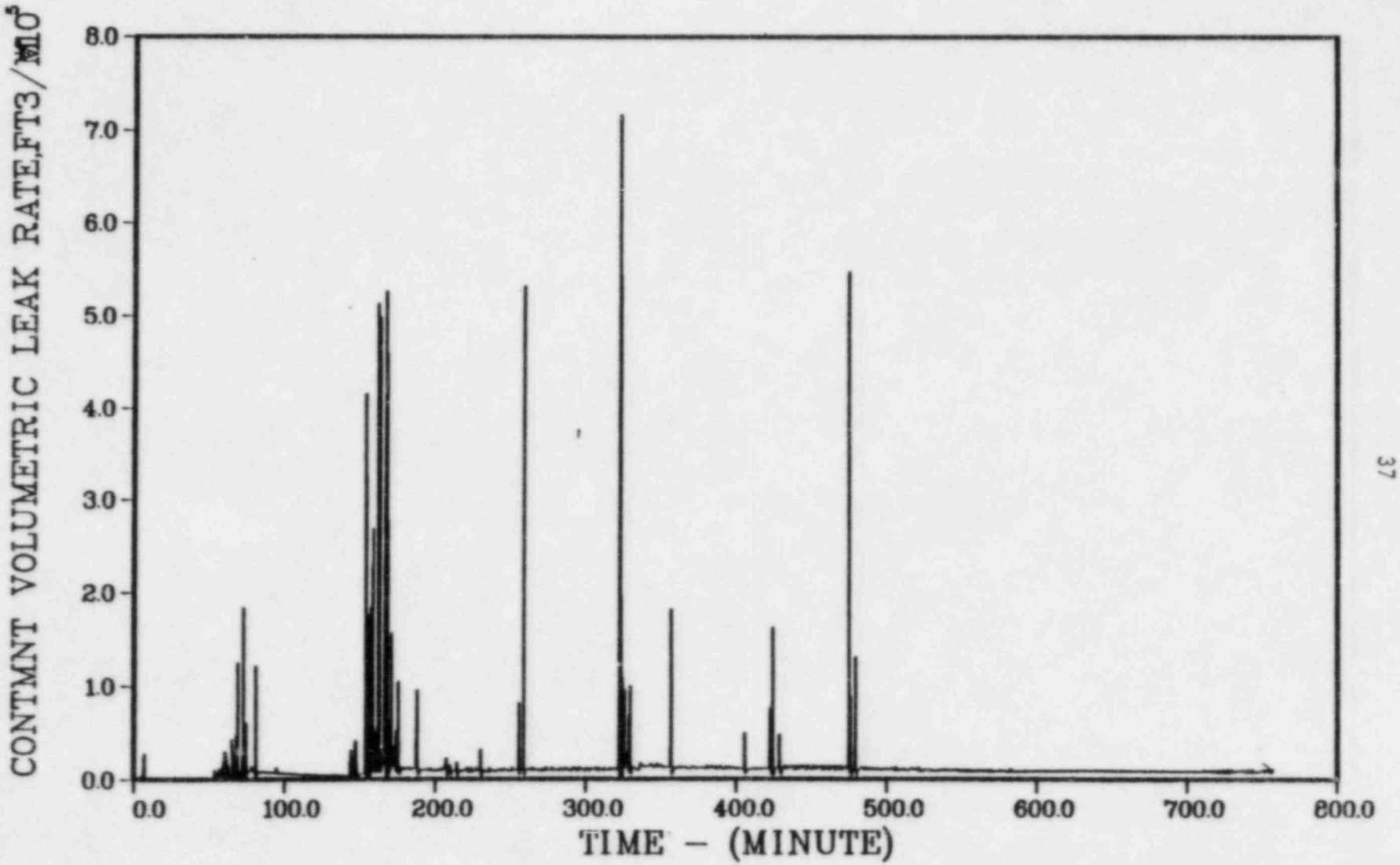

FIGURE 25. CONTAINMENT LEAK RATE FOR SEQUOYAH TMLB WITH ISOLATION FAILURE

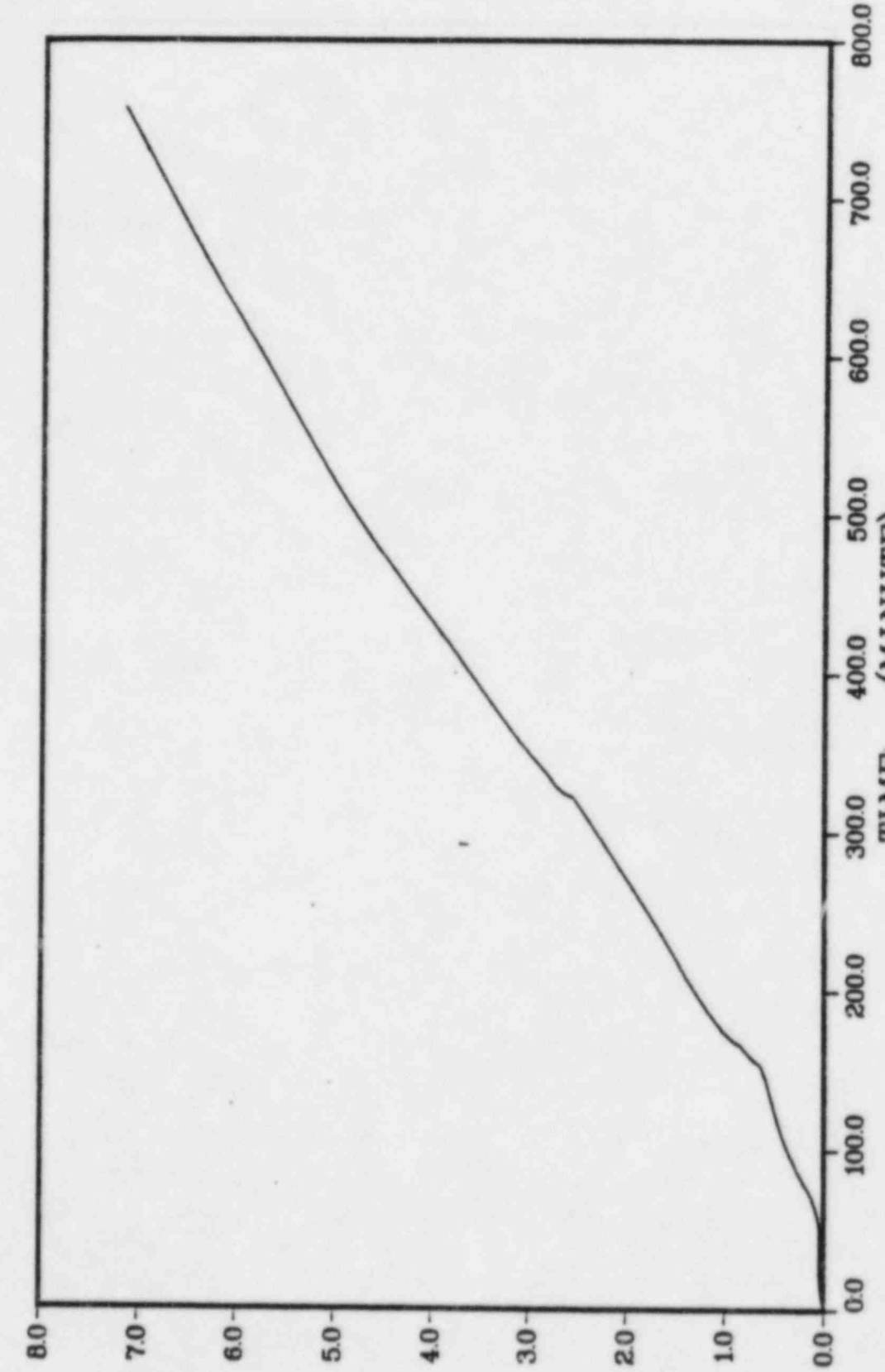

FIGURE 26. TOTAL LEAKAGE FOR SEQUOYAH TMLB WITH ISOLATION FAILURE

TABLE 8. LOCATIONAL DISTRIBUTION OF FISSION PRODUCTS FOR VARIOUS CONTAINMENT FAILURE MODES OF THE SEQUOYAH PLANT (TMLB')

Unit: Fraction of core inventory

Species	RCS	Lower Containment	Ice Bed	Upper Containment	Secondary Containment	Environment
			BMI-2104 (δ)			
CsI	0.82	8.6×10^{-3}	0.17	5.5×10^{-3}	--	3.9×10^{-4}
CsOH	0.83	5.4×10^{-2}	0.13	5.0×10^{-3}	--	4.5×10^{-4}
Te	0.25	0.91*	3.1×10^{-2}	3.8×10^{-3}	--	2.0×10^{-3}
			BMI-2104 (γ)			
CsI	0.82	6.1×10^{-2}	0.10	1.5×10^{-3}	--	1.7×10^{-2}
CsOH	0.83	3.9×10^{-2}	0.12	2.9×10^{-3}	--	2.3×10^{-2}
Te	0.25	0.70*	3.7×10^{-2}	6.2×10^{-4}	--	1.4×10^{-2}
			Isolation Failure			
CsI	0.82	4.9×10^{-2}	0.12	1.2×10^{-3}	7.8×10^{-3}	4.0×10^{-3}
CsOH	0.83	5.1×10^{-2}	0.11	1.2×10^{-3}	8.0×10^{-3}	4.3×10^{-3}
Te	0.25	0.69	3.7×10^{-2}	6.0×10^{-4}	5.9×10^{-3}	1.7×10^{-2}

*The number includes a fraction of 0.67 for Te not released from the core melt.

to the environment; a 6-inch diameter opening was selected to characterize the isolation failure.

The S_2E sequence (small break with failure of emergency core cooling) had been previously selected to investigate the possible effects of suppression pool bypass. This sequence was also chosen to investigate the consequences associated with containment isolation failure. For the present analyses, a normal suppression pool flow was assumed. Table 9 gives the accident event times for this sequence as they were determined in the BMI-2104 analyses. Figures 27 and 28 illustrate the containment pressure and temperature responses derived in the earlier analyses; the containment was predicted to fail due to the hydrogen burns taking place during the core slumping process. The reactor coolant system response for the containment isolation case was found to be substantially the same as had been previously evaluated. Thus for the present analyses, the release of fission products from the primary system was taken from the earlier analyses and only the containment transport of fission products was reevaluated.

Figures 29 and 30 illustrate the containment pressure and temperature responses determined for the present study. In the BMI-2104 analyses, the high containment pressures due to hydrogen burning were found to lead to containment failure; here, due to the presence of the preexisting leak, the pressures are not quite as high as previously observed. The hydrogen burning is seen to take place primarily in the drywell compartment of the containment. Figures 31 and 32 illustrate the containment leak rate and total leakage as determined in this study. The leak rate is seen to be sensitive to the pressures resulting from the hydrogen burns, as would be expected. The integrated leakage, however, increases smoothly with time. These containment responses were used as the basis for evaluating fission product release to the environment.

The results of the calculated fraction of core inventory released for CsI, CsOH, and Te are listed in Table 10. It is seen from the table that the release fractions for CsI and CsOH in the isolation failure mode are approximately half of the fractions for the BMI-2104 case, and release for Te is slightly lower than that for the BMI-2104

TABLE 9. ACCIDENT EVENT TIMES

Event	Time, minutes
	Grand Gulf S2E
Core Uncover	5.6
Start Melt	27.8
Hydrogen Burn	41.4
Start Slump	45.6
Hydrogen Burn	54.4
Containment Fail	54.4
Core Collapse	57.6
Hydrogen Burn	57.6
Hydrogen Burn	59.6
Vessel Head Dry	80.7
Head Fail	119.2
Concrete Attack	119.2
Hydrogen Burn	125.6
Cavity Dry	213.7
Hydrogen Burn	245.5
End Calculation	720.3

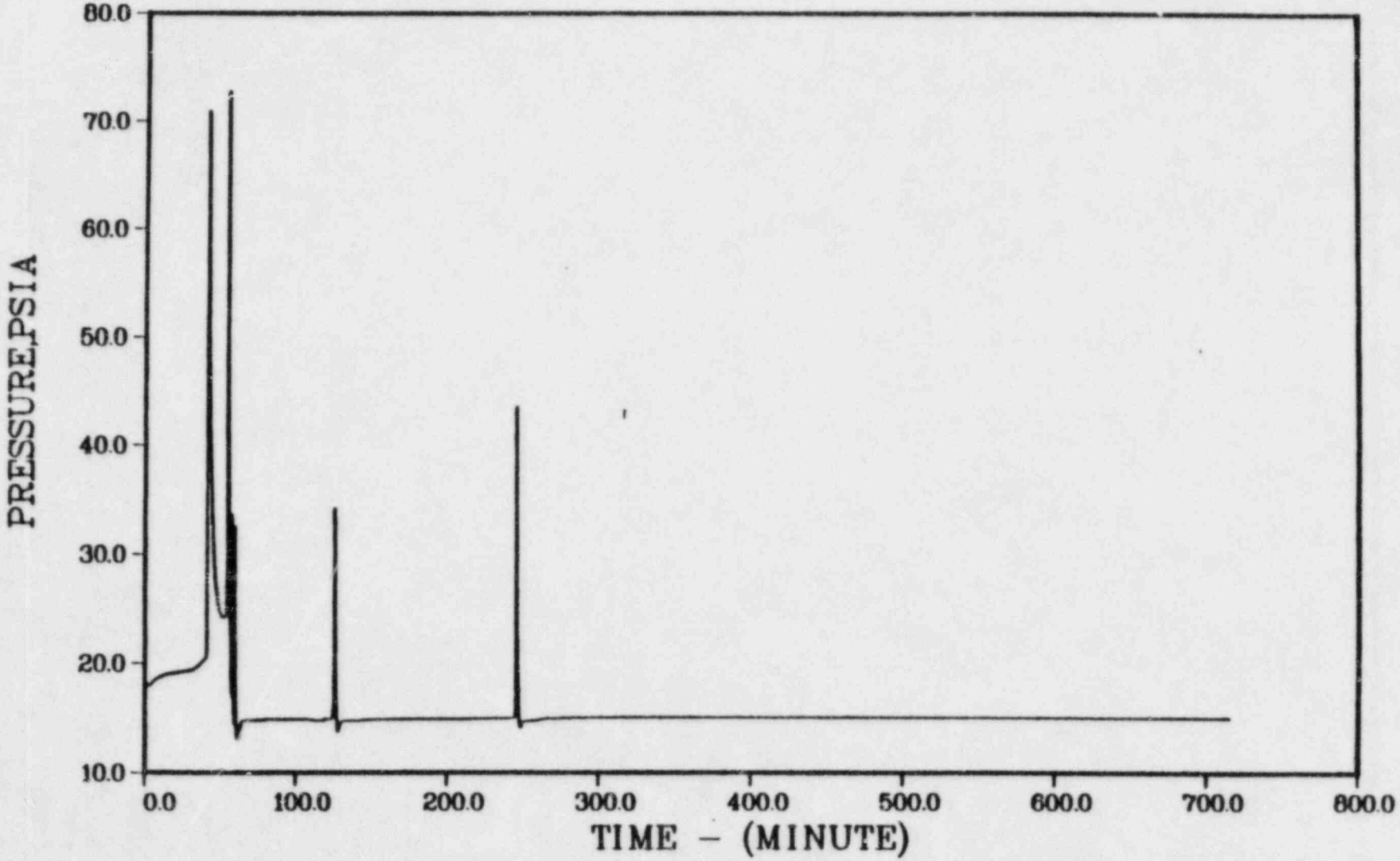

FIGURE 27. CONTAINMENT PRESSURE WITH NOMINAL POOL BYPASS FOR GRAND GULF (SEQUENCE S_2E)

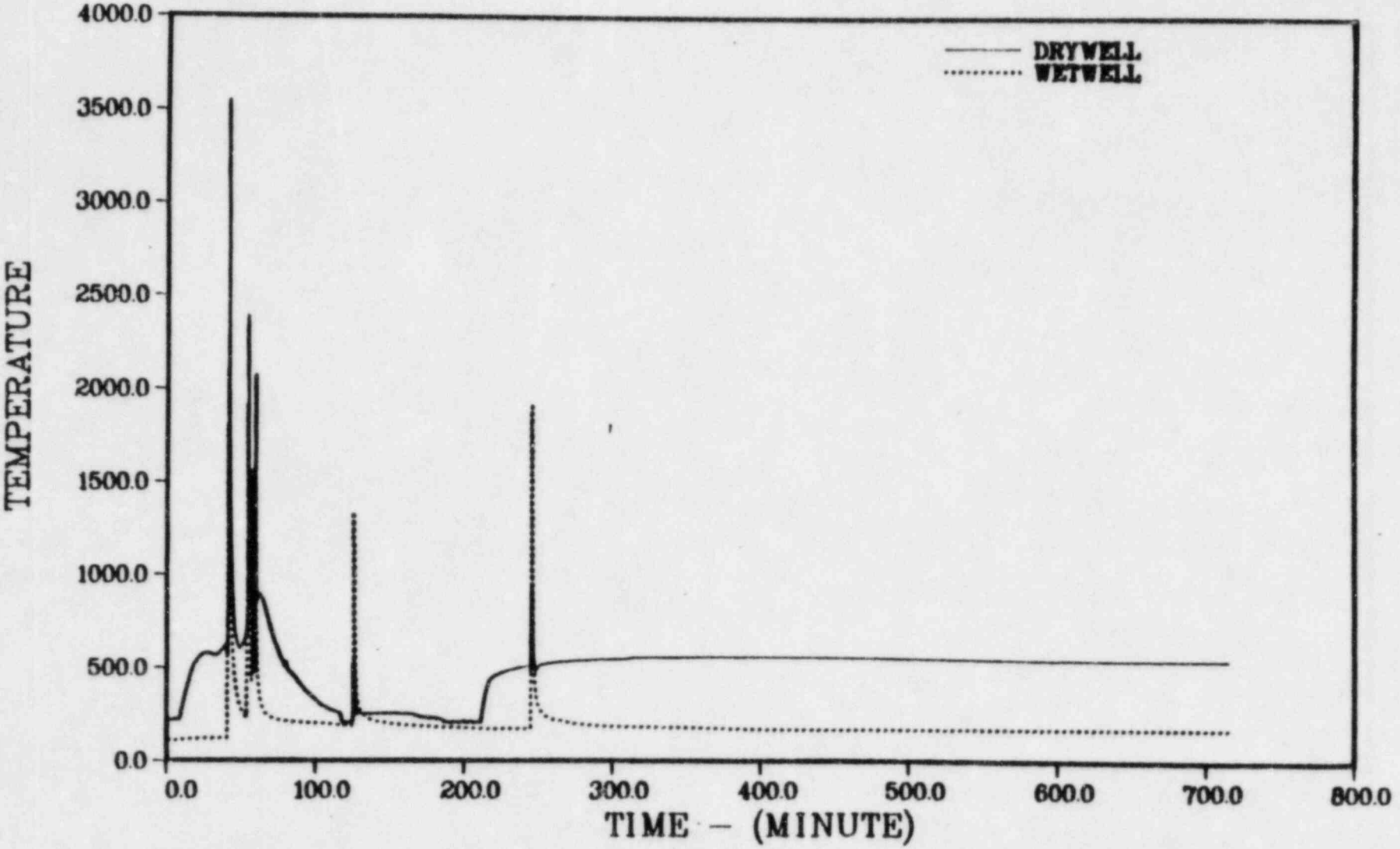

FIGURE 28. CONTAINMENT TEMPERATURES WITH NOMINAL POOL BYPASS FOR GRAND GULF (SEQUENCE S_2E)

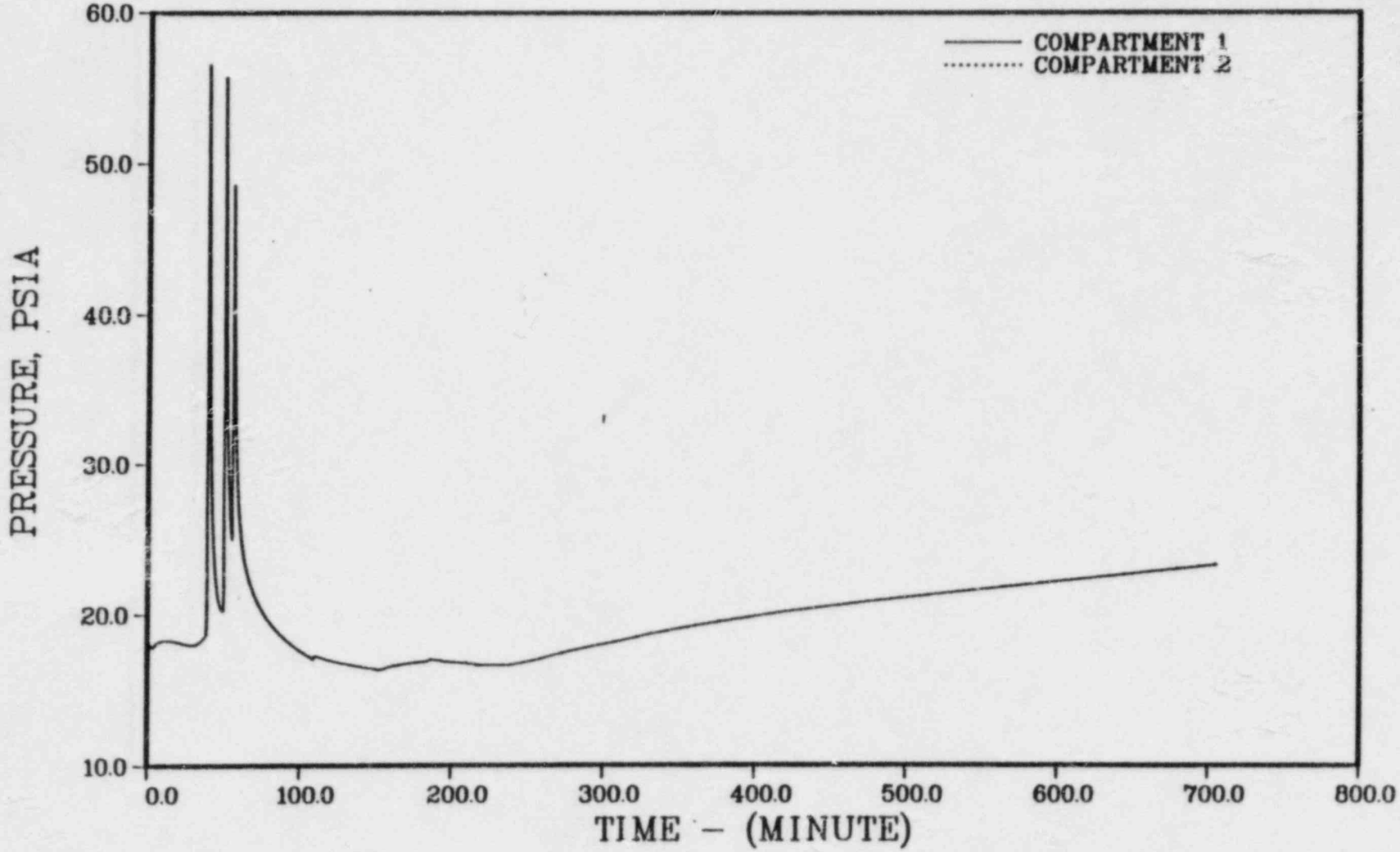

FIGURE 29. CONTAINMENT PRESSURE RESPONSE FOR GRAND GULF S_2E WITH ISOLATION FAILURE

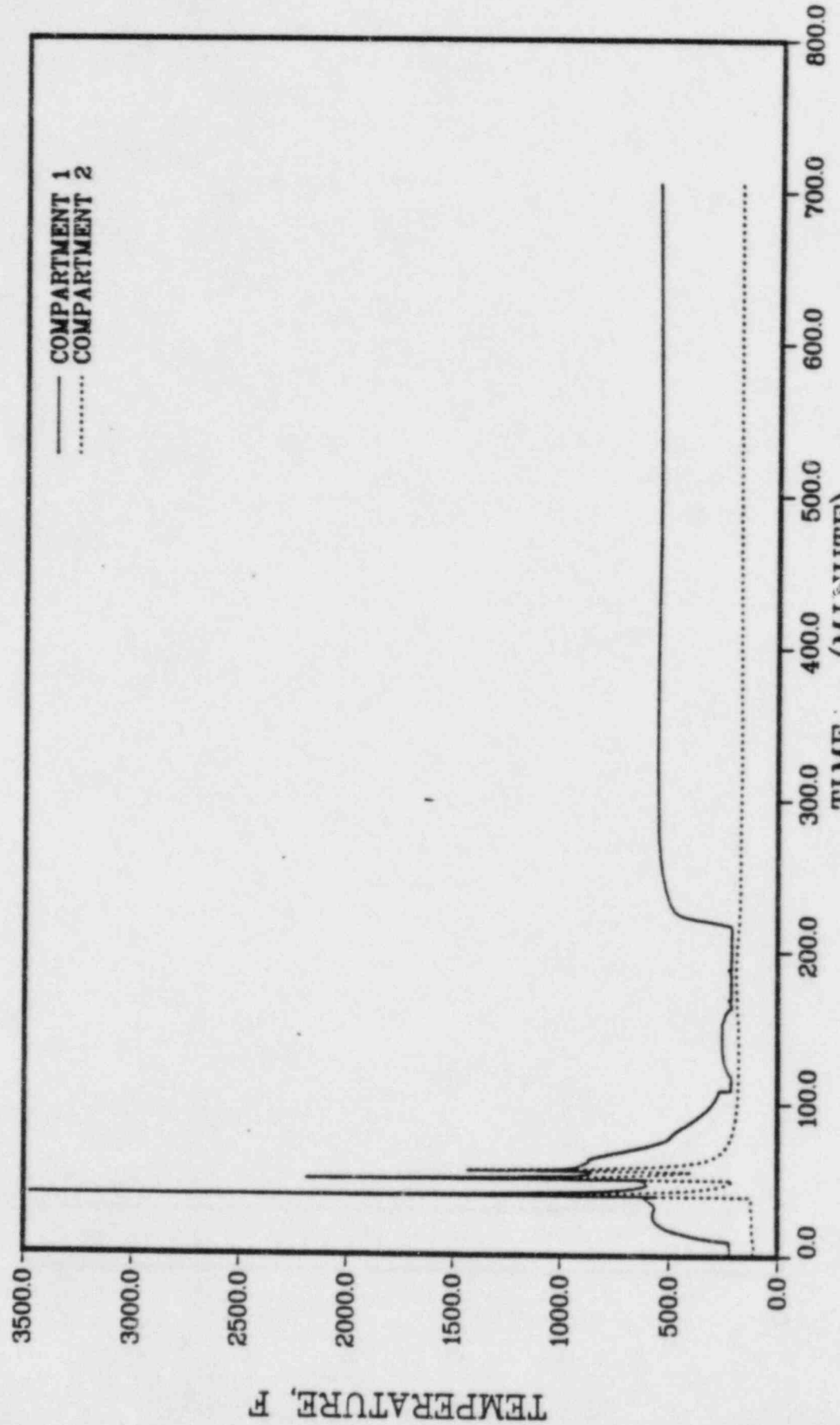

FIGURE 30. CONTAINMENT TEMPERATURE RESPONSE FOR GRAND GULF S_2E WITH ISOLATION FAILURE

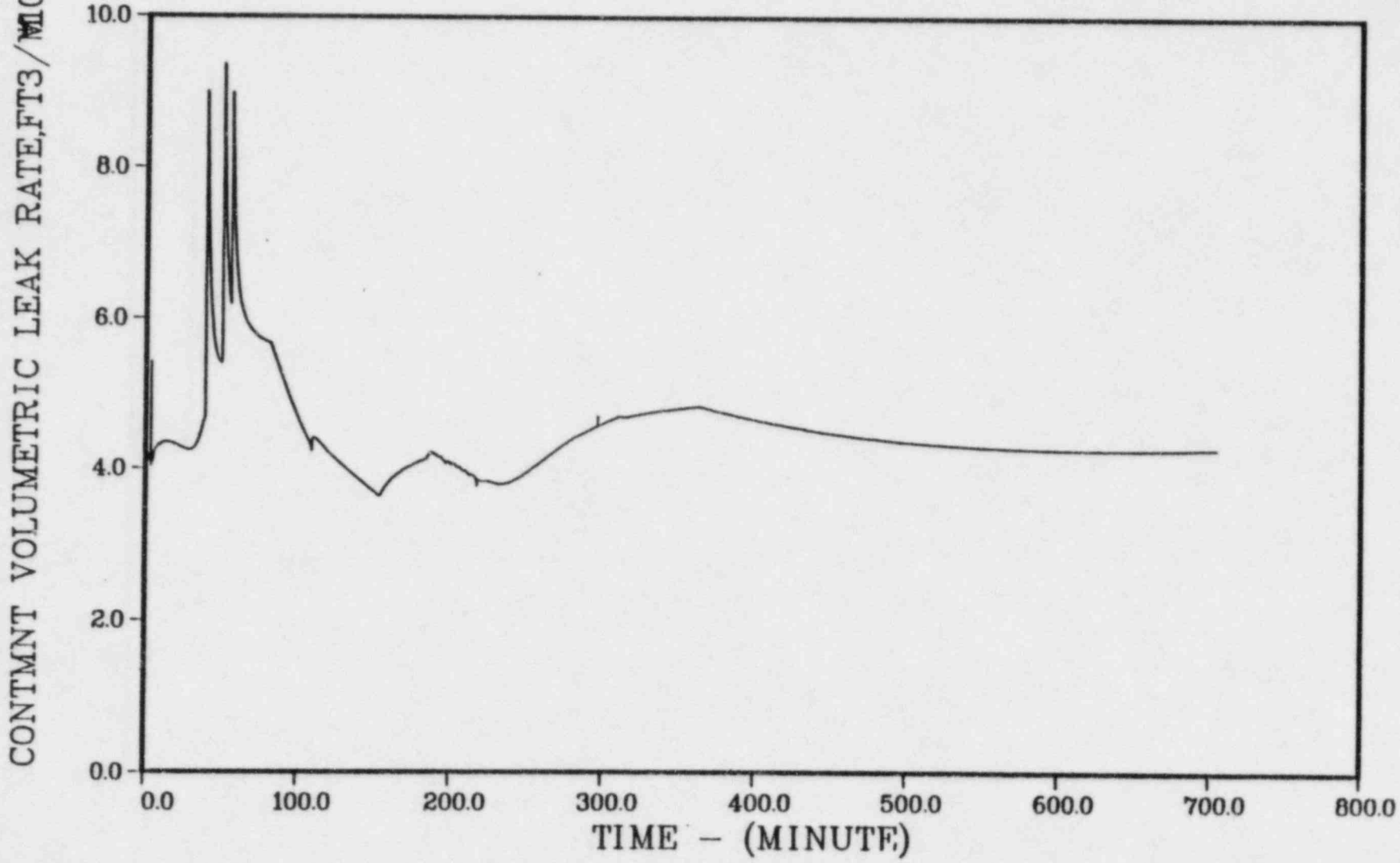

FIGURE 31. CONTAINMENT LEAK RATE FOR GRAND GULF S_2E WITH ISOLATION FAILURE

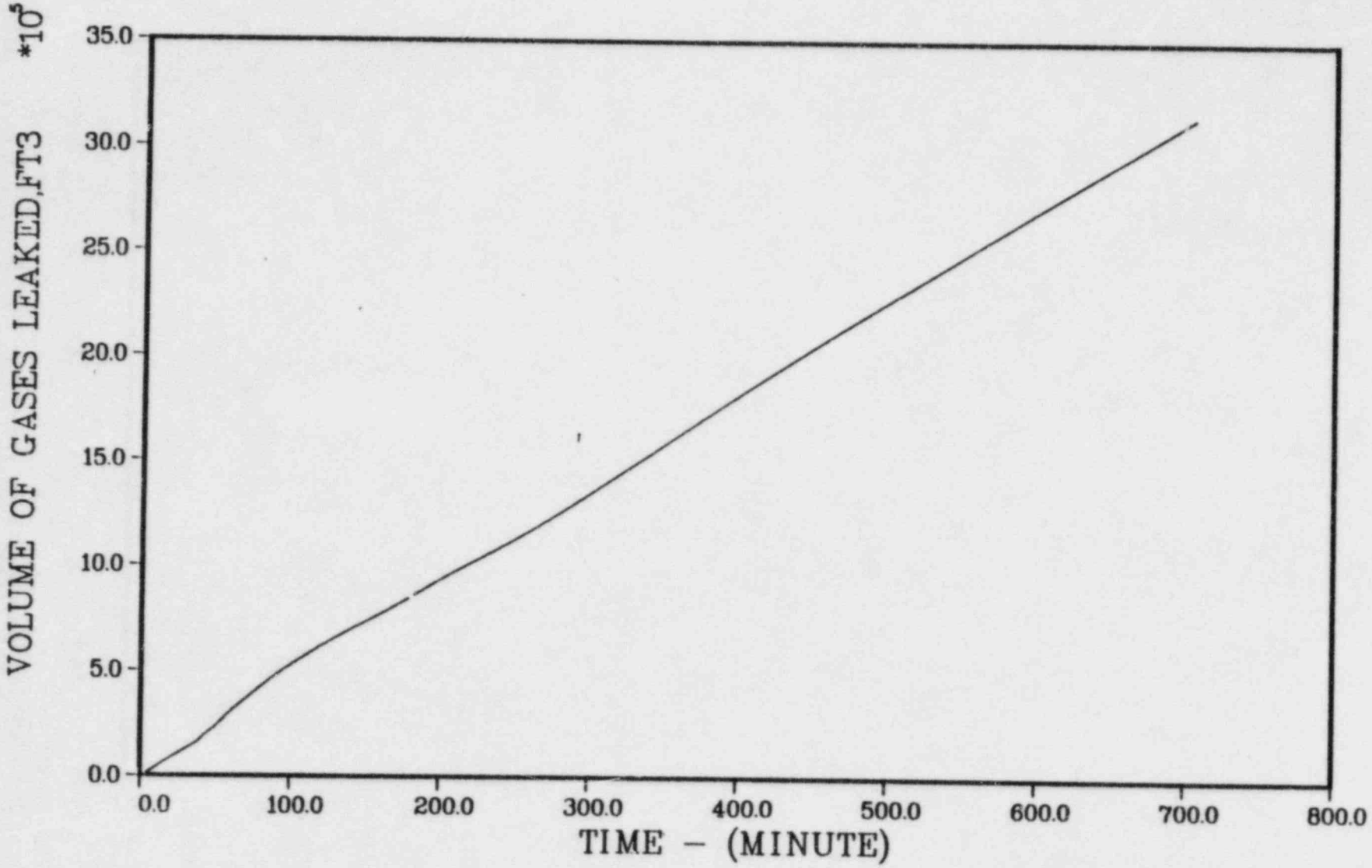

FIGURE 32. TOTAL LEAKAGE FOR GRAND GULF S_2E WITH ISOLATION FAILURE

TABLE 10. LOCATIONAL DISTRIBUTION OF FISSION PRODUCTS FOR VARIOUS CONTAINMENT FAILURE MODES OF THE GRAND GULF PLANT (S_2E)

Unit: Fraction of core inventory

Species	RCS	Drywell	Suppression Pool	Containment	Environment
			BMI-2104		
CsI	9.1×10^{-2}	1.2×10^{-2}	0.89	9.6×10^{-4}	7.0×10^{-3}
CsOH	0.16	1.1×10^{-2}	0.82	8.6×10^{-4}	6.3×10^{-3}
Te	0.26	0.39*	0.11	6.5×10^{-3}	2.4×10^{-2}
			Isolation Failure		
CsI	9.1×10^{-2}	1.1×10^{-2}	0.89	2.5×10^{-3}	3.8×10^{-3}
CsOH	0.16	1.0×10^{-2}	0.82	2.2×10^{-3}	3.5×10^{-3}
Te	0.26	0.40*	0.30	1.5×10^{-2}	2.0×10^{-2}

*The number includes a fraction of 0.355 for Te not released from the core melt.

case. Again, the decreased leakage rate to the environment in the isolation failure is largely responsible for the observed reductions.

Peach Bottom -- Mark I BWR

For the Peach Bottom BWR which has a Mark I pressure suppression design, the failure of the containment to isolate at the start of the accident was selected as the representative noncatastrophic containment failure mode. The isolation failure was assumed to be a 6-inch diameter opening in the drywell of the containment, and the leakage through it was assumed to go the secondary containment building. The TC sequence (transient with failure to scram) was used as the basis for these analyses.

The TC sequence was one of the accidents treated in BMI-2104, Volume II, for the Peach Bottom design, including consideration of the effect of the secondary containment. Table 11 gives the accident event times for this sequence as calculated in the earlier study. Figures 33 and 34 illustrate the containment pressure and temperature responses in the primary containment from the earlier analyses. Figure 35 gives the pressure history in the secondary containment as predicted under the assumptions of the earlier study. With regard to the predicted secondary containment response, it should be noted that it was based on a constant Standby Gas Treatment System (SGTS) exhaust rate of 25,000 cubic feet per minute and utilized the entire volume of the reactor building. Even with these assumptions the secondary containment was pressurized for a considerable period of time, leading to substantial leakage from the building that did not pass through the SGTS.

Under the BMI-2104 assumptions for the TC sequence, containment failure precedes core melting, with the imbalance between heat input and removal to the containment leading to pressurization and failure. In the containment isolation failure case considered here, the containment is "failed" at the start of the accident and the timing of the entire accident sequence could be different from the case previously considered. Thus there is some conceptual difficulty in doing a comparable evaluation. In order to circumvent this difficulty, the failure of the emergency

TABLE 11. ACCIDENT EVENT TIMES

Event	Time, minutes
	Peach Bottom TCY
Containment Heat Removal On	10.0
Containment Fail	58.1
ECC Recirculation On	72.4
ECC Off	72.6
Core Uncover	73.0
Start Melt	93.6
Core Slump	124.6
Bottom Head Dry	136.6
Core Collapse	178.9
Bottom Head Fail	216.6
Reactor Cavity Dry	216.7
Start Concrete Attack	216.7
End Calculation	816.9

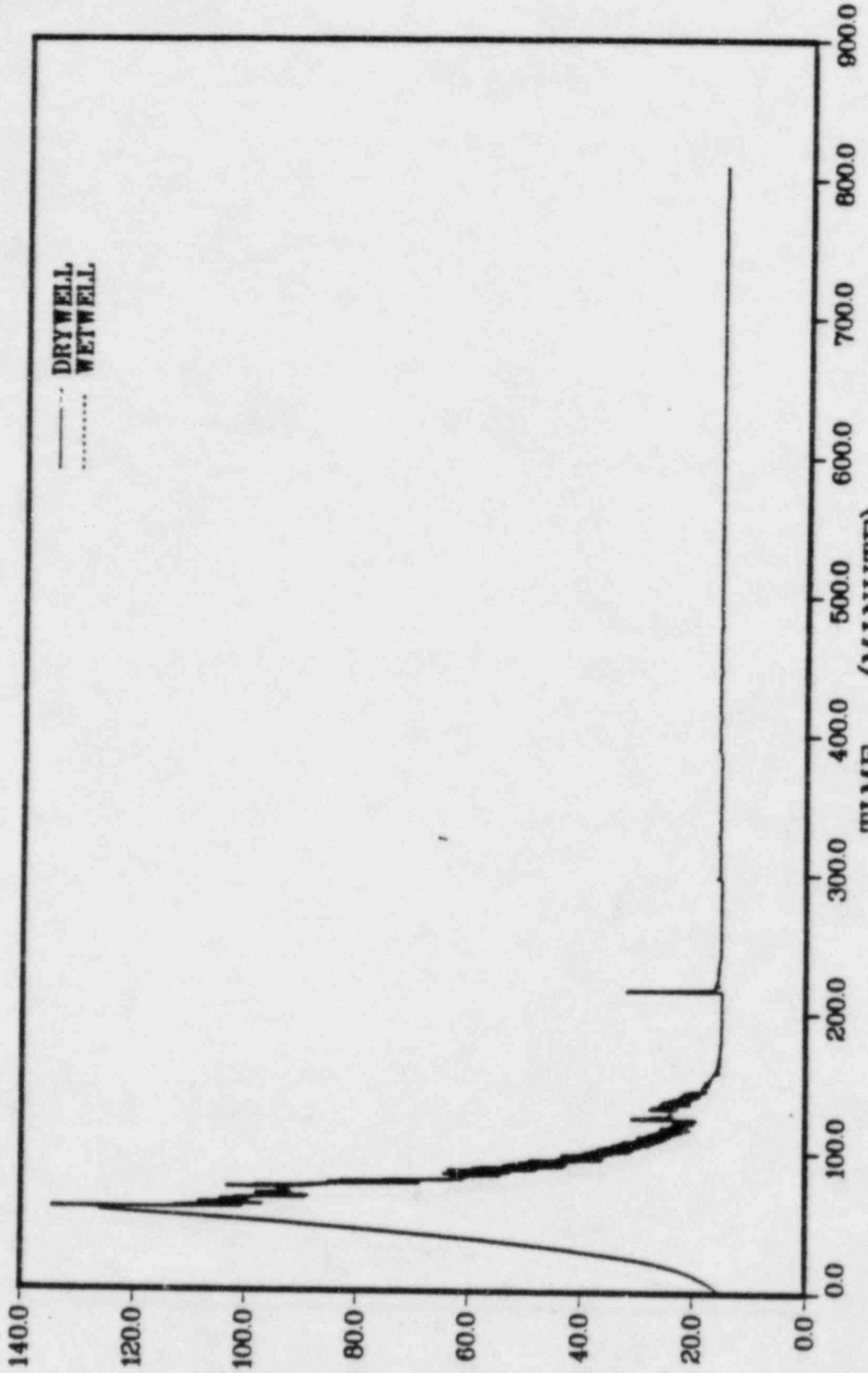

FIGURE 33. PRESSURES IN CONTAINMENT VOLUMES (SEQUENCE TC)

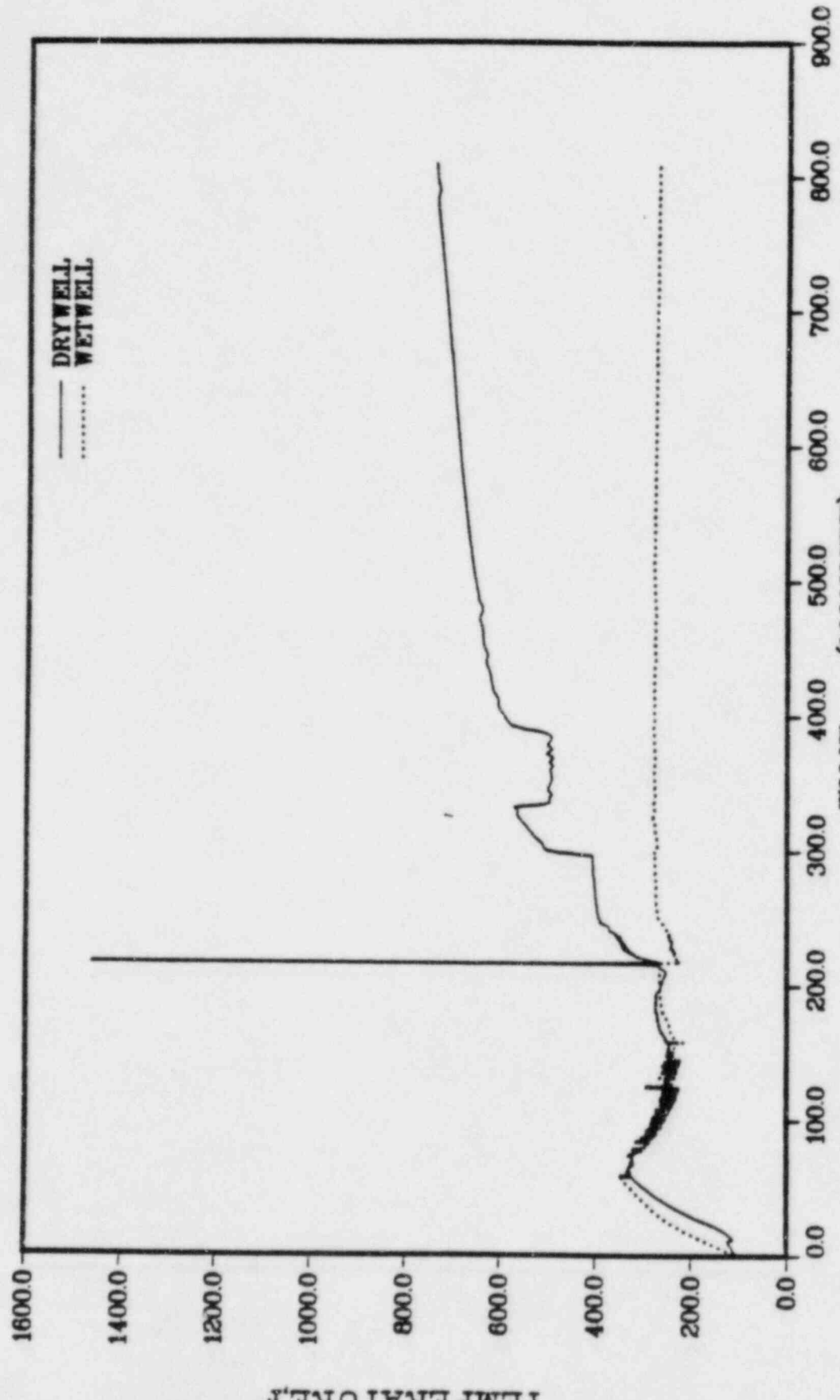

FIGURE 34. GAS TEMPERATURES IN CONTAINMENT VOLUMES (SEQUENCE TC)

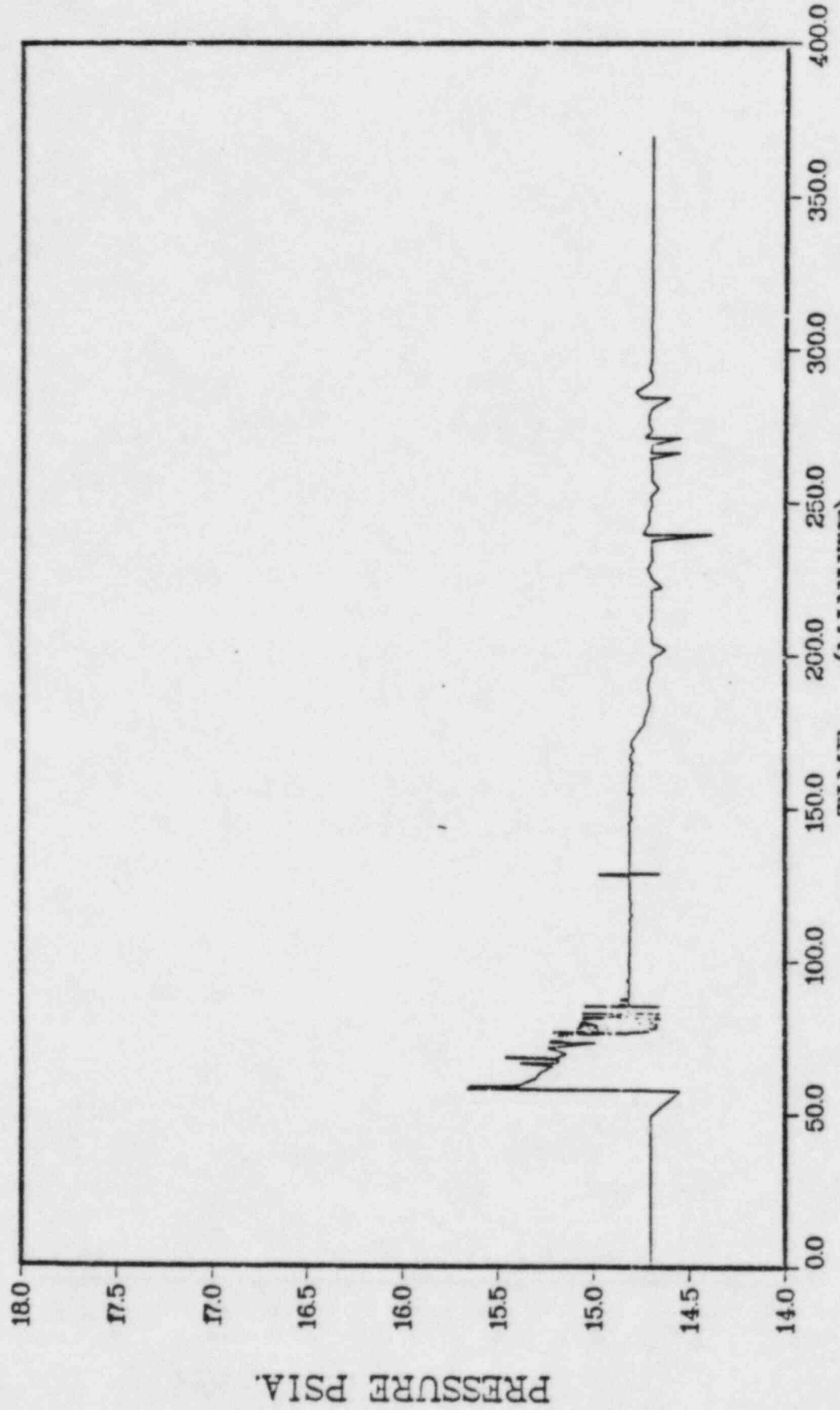

FIGURE 35. REACTOR BUILDING PRESSURE DURING TC-Y' SEQUENCE

core cooling system for the containment isolation failure case was assumed to take place at the same time as in the earlier analyses. With this assumption and primary system treatment consistent with the earlier analyses, it was found that a 6-inch opening in the containment was not able to keep up with the steam input to the suppression pool and that the containment was predicted to pressurize above the failure level assumed in the earlier analyses. The containment pressure response for the above containment isolation failure case but with no overpressurization failure allowed is illustrated in Figure 36.

Additional containment calculations were performed utilizing larger initial isolation failures; the results of these calculations indicated that initial hole sizes of several square feet in area would be required to maintain the primary containment pressure below the failure level. The foregoing observations are quite consistent with containment venting investigations conducted in the past in which it had been found that rather substantial openings (3 feet diameter) were required to keep up with the steam generation in sequences of the type considered here. Based on these observations, it is concluded that for the nominal containment isolation failure hole size of 6 inches employed in these analyses the containment still would overpressurize and fail with the result that the accident sequence is nearly identical to the TC case considered in BMI-2104. Of course, other hole size assumptions could be made but a large initial opening would be required to prevent excessive pressure loads. In either case the environmental fission product source terms would not be expected to differ appreciably from the previous results for this TC sequence in which the containment was assumed to be initially intact but was predicted to fail by overpressurization. The particular case of interest is designated TC-γ in Volume II of BMI-2104 and since the isolation failure case considered is essentially identical, the results for TC-γ are shown in Table 12 to indicate this equality between the two assumptions.

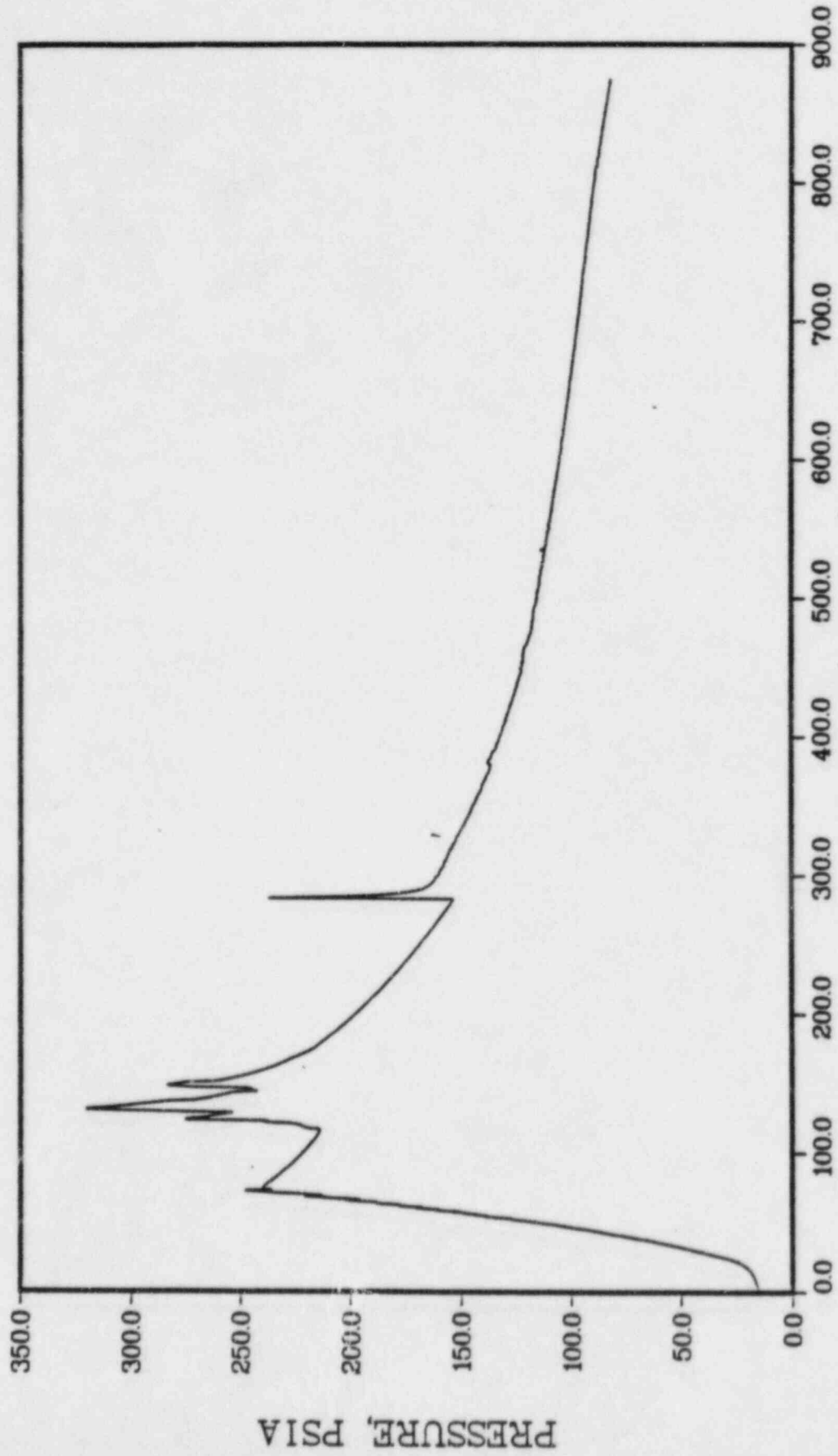

FIGURE 36. CONTAINMENT PRESSURE RESPONSE FOR PEACH BOTTOM TC SEQUENCE WITH ISOLATION FAILURE

TABLE 12. LOCATIONAL DISTRIBUTION OF SPECIES OF THE PEACH BOTTOM PLANT
(TC-γ and TC-Isolation Failure)

	Fraction of Core Inventory						
Species	RCS	Pool	Drywell	Wetwell	Reactor Bldg	SGTS	Environment
CsI	0.06	0.69	1.5×10^{-2}	0	6.9×10^{-2}	6.8×10^{-2}	0.10
CsOH	0.22	0.56	1.4×10^{-2}	0	6.1×10^{-2}	5.8×10^{-2}	9.1×10^{-2}
Te	0.34	7.9×10^{-3}	0.29*	0	0.11	1.3×10^{-2}	0.25

*This includes a fraction of 0.13 for Te which is found not to be released from the core-concrete interaction.